Expression of AKT/PKB, PTEN and CLOCK in Merkel cell carcinoma cell lines

submitted by

Monika, Breuer, Dipl. Ing.in (FH)

for the award of the academic degree

Doktorin der gesamten Heilkunde

(Dr.in med. univ.)

at the

Medical University of Graz

Thesis supervisors

Sattler, Wolfgang, Ao.Univ.-Prof. Mag. Dr.rer.nat.

Department of Molecular Biology and Biochemistry

at the Medical University of Graz

Becker, Jürgen, Univ. Prof. Dr.

Department of Translational Skin Cancer Research,

German Consortium for Translational Cancer Research

Essen/Düsseldorf

Graz, 29.01.2018

Statutory Declaration

“I declare in lieu of an oath that I have written this diploma thesis myself and that I have not used any sources or resources other than stated for its preparation. I further declare that I have clearly indicated all direct and indirect quotations. This diploma thesis has not been submitted elsewhere for examination purposes.”

Graz, 29.01.2018 *Monika Breuer eh.*

Acknowledgement

Special thanks for supporting my thesis work go to Vishwanath Bath Kumble who has not only an impressive attitude to life but also excellent teaching skills.

Moreover, the possible reason for his skills and knowledge, our supervisor Wolfgang Sattler whom I would like to thank for his good advices, his efforts and kindness.

Furthermore, I`m grateful for the support of Linde and Ludwig Breuer, Johan, Henri E. and Isabella Vinzelberg, Gertrude and Johannes Schleich, Elke and Ulrich Vinzelberg.

I feel the utmost urge to say a thousand thanks to Katrin Klepeis, Nikola V. Leitgeb, Biljana Budes, Sylvain Boursier, Jonna Heikinnen and Michael P. Bailey who let me see life in the most exciting and brightest colors.

Also, I would like to thank Jürgen Becker for the opportunity to spend time working in an interesting lab environment.

Importantly for the quality time thanks to Vishwanath Bath Kumble, Ivelina Spassova, Kashif Rasheed, Shahlo Muminova, Corinna Wülbeck and Kaiji Fan.

Since this is an Austrian based work, please forgive me not listing all your titles and achievements.

Table of Content

List of Figures

List of Tables

List of Abbreviations

Ab	antibody
AKT	v-akt murine thymoma viral oncogene homolog
AMPK	5‘ adenosine monophosphate-activated protein kinase
APUD	amine precursor uptake decarboxylase
ARNTL1	gene name of BMAL1
ATM	ataxia telangiectasia mutated
ATR	ATM and Rad3-related
BAD	BCL2 antagonist of cell death
BMAL	brain and muscle, ARNT-like
CDK	cyclin-dependent kinase
CE	cytoplasmic/cytosolic extraction
CHK	checkpoint kinase
Cip	CDK-interacting protein
CK	cytokeratin
CK1δ/ε	casein kinase1δ/ε
CLOCK	circadian locomotor output cycles kaput
c-Myc	myelocytomatosis viral oncogene homolog
CRY	cryptochrome
DNA	desoxyribonucleic acid
E-box	enhancer box
E2F	E2 promoter binding factor
FCS	fetal calf serum
FOXO	forkhead box protein O
G1	gap 1 phase
HRP	horse radish peroxidase
HS	heat shock
IgG	immunoglobulin G
IL2rγ^{null}	null mutation in interleukin-2 gamma chain receptor
INK	inhibitor of cyclin-dependent kinase
Kip	kinase inhibitor protein

LTAg	large T antigen
LOH	loss of heterozygosity
M	mitosis
mAb	monoclonal antibody
MCC	Merkel cell carcinoma
MCPyV	Merkel cell polyomavirus
MDM2	mouse double minute 2 homolog
MMAC1	mutated in multiple advanced cancers 1
mRNA	messenger ribonucleic acid
MZK	Merkelzellkarzinom
MzPyV	Merkelzellpolyomavirus
N/C	nuclear/cytosplasmic
NAD^+	nicotinamide adenine dinucleotide (oxidized form)
NAMPT	nicotinamide phosphoribosyltransferase
NOD	non-obese diabetic
NR1D1,2	gene names of REV-ERBα and β
NSG	NOD/SCID/IL2rγ^{null}
p	tumor protein
P	phosphate
PCR	polymerase chain reaction
PER	period
P/S	penicillin/streptomycin
PCR	polymerase chain reaction
PDK	phosphoinositide-dependent kinase
PI3K	phosphatidylinositol 3-kinase
PIK3CA	phosphatidylinositol-4,5-bisphosphate 3-kinase catalytic subunit α
PIP_3	phosphatidylinositol (3,4,5) -triphosphate
PtdIns (3,4,5) P_3	phosphatidylinositol (3,4,5) -triphosphate
PTEN	Phosphatase and Tensin homolog deleted on chromosome Ten
Rb	retinoblastoma protein
REV-ERB α, β	reverse erythroblastosis virus α, β
ROR	retinoic acid-related orphan receptor

RRE	R-response element
RTK	receptor tyrosine kinase
S	synthesis phase
SCID	severe combined immune deficient
SCN	suprachiasmatic nucleus cells
SDS	sodium dodecyl sulfate
Ser	serine
shRNA	short hairpin ribonucleic acid
siRNA	small interfering ribonucleic acid
SIRT1	sirtuin1
TAg	tumor antigen
T/E	trypsin/EDTA
TIM	timeless
UM	University of Michigan
UV	ultraviolet
WB	Western blot/blotting
WP	whole protein

Zusammenfassung

Fehlfunktion oder Mutation des bedeutenden Tumorsuppressors *Phosphatase and Tensin homolog deleted on chromosome Ten* (PTEN) ist impliziert mit der Pathogenese einer Vielfalt von Karzinomen. Ein solcher Zusammenhang konnte für die Tumorgenese des Merkelzellkarzinoms (MZK) noch nicht demonstriert werden; MZK ist ein höchst aggressives und seltenes kutanes neuroendokrines Karzinom mit dürftigen therapeutischen Aussichten. Nichtsdestotrotz, die Entdeckung des Merkelzellkarzinompolyomavirus (MZPyV) war ein enormer Schritt hin zur Erforschung zugrundeliegender Pathogenesemechanismen. Ob das MZPyV die Kopplung des molekularen zirkadianen Zyklus mit dem Zellzyklus zugunsten viraler Transkription hinsichtlich einer zirkadian/zellulär gekoppelten Weise verändert, ist eine Hypothese die es wert ist zu ergründen bezüglich möglicher Chronotherapieansätze.

Das Ziel dieser Arbeit ist herauszufinden, ob MZPyV-positive MZK die PTEN-Expression bestimmen wie auch die Aktivierung/Phosphorylierung von AKT verglichen mit MZPyV-negativen MZK Zelllinien.

Hinsichtlich Western blotting wurden ganze Zelllysate von vier MZPyV-negativen Zelllinien sowie neun MZK Zelllinien, welche virale DNA aufweisen, untersucht, mit der Verwendung von primären Antikörpern, gerichtet gegen PTEN, pAKT^{S473}, AKT und β-Tubulin als Ladekontrolle. Alle untersuchten Zelllinien exprimieren PTEN, jedoch konnte kein signifikanter Unterschied hinsichtlich MZPyV-Status festgestellt werden. pAKT ^{S473}-Level zeigen sich höchst variabel unter den Zelllinien und mit deutlich geringerer Expression.

Zusätzlich wurden nukleäre und zytoplasmatische als auch ganze Zelllysate von hitzegeschockten oder unbehandelten/unsynchronisierten MZPyV-positiven WaGa Zellen untersucht, um die subzelluläre Lokalisation von PTEN zu bestimmen sowie eine Kolokalisation von CLOCK. Dabei wurden primäre Antikörper spezifisch für PTEN und CLOCK sowie β-Actin und β-Tubulin als Zytosolkontrollen und Lamin B1 als Nukleuskontrolle eingesetzt. PTEN und CLOCK wurden einzig im Nukleus detektiert.

Trotz der deutlichen Evidenz einer PTEN Aktivierung bezüglich totaler Zelllysate aller dreizehn MZK Zelllinien sowie des experimentellen Designs nukleäre und zytosolische Extraktion hinsichtlich WaGa Zellen; könnte dieser etablierte experimentelle Aufbau als solide und verlässliche Basis für weiterführende Untersuchungen dienen um von MZPyV potentiell beeinflusste Mechanismen in Verbindung mit dem zirkadianen Zeitsystem und der Modulation von Zellwachstum aufzudecken.

Abstract

Loss or alterations of the prominent tumor suppressor *Phosphatase and Tensin homolog deleted on chromosome Ten* (PTEN) is clearly implicated with the pathogenesis of a variety of cancers. This association has not yet been demonstrated for the tumorigenesis of Merkel cell carcinoma (MCC); a highly aggressive and rare cutaneous neuroendocrine carcinoma with poor therapeutic options. Nevertheless, the discovery of the Merkel cell polyomavirus (MCPyV) was an enormous step towards revealing underlying mechanisms of its pathogenesis. Whether MCPyV alters the coupling of the molecular circadian cycle to the cell cycle in order to favor viral transcription in a circadian/cellular cycle fixed manner is a hypothesis worth to be explored in respect to a potential chronotherapeutic approach.

The aim of this thesis is to clarify whether MCPyV-positive MCC determines expression levels of PTEN as well as activation/phosphorylation of AKT in comparison to MCPyV-negative MCC cell lines.

For western blotting, total cell lysates of four MCPyV-negative cell lines, as well as nine MCC cell lines which harbor viral DNA, were investigated by employing primary antibodies targeted against PTEN, pAKT^{S473}, AKT and β-Tubulin as a loading control. Revealing that all cell lines tested express PTEN but without significant differences regarding MCPyV status. pAKT ^{S473} levels are highly variable amongst the cell lines and by far expressed at a lesser extent.

Additionally, to characterize the subcellular localization of PTEN and to evaluate Clock's colocalization, nuclear and cytosolic as well as total cell lysates of MCPyV-positive WaGa cells of either heat-shocked or untreated/desynchronized samples were used to be probed with primary antibodies specific for Clock and PTEN; as well as β-Actin and β-Tubulin as cytosolic controls and Lamin B1 as nuclear loading control. PTEN and Clock were detected solely in the nucleus.

Despite the clear evidence of PTEN activation concerning total cell lysates of all thirteen MCC cell lines as well as for the experimental design nuclear and cytosolic extraction regarding WaGa cells; this established experimental set-up could provide a solid and reliable basis for further experiments to elucidate

mechanisms relating to the circadian timing system and modulation of cell growth potentially exploited by MCPyV.

1 Introduction

1.1 The Merkel cell carcinoma

In 1972, the pathologist Cyril Toker described for the first time five unusual cutaneous carcinomas of five patients showing uniform morphology. These had a trabecular or lattice-like infiltrative growth pattern with nests of cells located in the dermis of the skin on histological observation, which later were classified as Merkel Cell Carcinoma (MCC).[1,2] This tumor usually spreads into the reticular dermis and subcutis but not into the papillary dermis, epidermis and adnexa.[3] Toker named or classified those malignant lesions, which cancer cells have already disseminated by lymphatic vessels, '*trabecular carcinoma of the skin*'.[1,2] In the meanwhile it is evident that the trabecular type is just one out of three distinct types of these carcinomas based on histological differentiation. Interestingly, together with the small-cell type, which also occurs in around 10% of cases, it is quite rare. In approximately 80% of cases, the intermediate type is the most frequent one. However, also mixed as well as transitional forms are occurring quite frequently.[3]

The origin of the 'trabecular carcinoma of the skin' was still unclear. In 1978, Tang and Toker set the stage for a change or a rethinking; which reflect in a renaming of this specific type of skin carcinoma based on their underlying electron microscopic studies. Their findings of dense-core granules, regarding three tumors, having similar morphology as cells differentiating from neurocrest or APUD (Amine Precursor Uptake Decarboxylase) cells suggested that the trabecular carcinoma of the skin might be derived from cells of neurocrest origin.[4] Other synonyms for the MCC are therefore APUDoma of the skin and small-cell neuroepithelial tumor of the skin.[5]

Furthermore, melanosomes or premelanosomes could not be identified; the choice for a specific search was quite reasonable since melanoblasts could have been a possible suspect of origin as being neurocrest derivatives.[4] Another candidate, the Merkel cells, were first described by Friedrich Sigmund Merkel in 1875 as 'Tastzellen' (touch cells), as a reference to their somatosensory function as slowly adapting mechanoreceptors within the skin.[3,6] They are located in the basal layer or stratum basale of the epidermis; thus assembled in large numbers in eccrine glandular ridges of glabrous skin as well as in hair discs, within belt-like clusters of hair follicles and in certain mucosal tissues.[6] Moreover, Tang and Toker recognized that they showed strong

similarities at ultrastructural level with the tumor cells under investigation. The Merkel cells exhibited electron-dense neurosecretory type granules indistinguishable from those found in neurocrest derivatives; therefore MCC is classified as a neuroendocrine skin carcinoma.[4] Nowadays, it is known that Merkel cells are the only cells which form such granules.[7] Nonetheless, Tang and Toker stated that "the trabecular carcinoma is derived from neurocrest, most probably Merkel cell" or they share a common precursor.[4,8] Even until now the definite origin of Merkel cell carcinoma is an unresolved and controversial question, and a topic for further research studies. The most recent hypothesis suggests that MCC might originate from early pre/pro- or pre-B-cells, which have the ability to differentiate into different cell types.[9] This is based on the assumption of descriptive data obtained by employing immunohistochemistry as well as molecular data.[10]

Importantly, immunohistochemical staining is required for a definite diagnosis, which shows characteristic perinuclear globule upon staining for low-molecular-weight cytokeratin's (CK) such as CK 20, CK 5/5 and CK 7.[2,8] Additionally, neuroendocrine markers such as neural cell adhesion molecule (NCAM/cluster of differentiation CD56), chromogranin A and synaptophysin are expressed by all distinctive MCC subtypes.[9] In routine immunohistochemical diagnosis, CK 20 is quite specific but not always positive. A staining for the neuroendocrine marker neuron-specific enolase (NSE) is in contrast usually positive but relatively unspecific.[3] Therefore to rule out differential diagnosis of morphologically similar entities such as metastatic extra-cutaneous small cell carcinoma and to confirm the previous staining results, further stains are performed for thyroid transcription factor 1 (TTF 1), leukocyte common antigen (LCA) and vimentin, which are usually negative.[3,11]

Further research effort in the field of MCC regulatory pathways and thus finding effective therapeutic strategies is necessary and important. This is due to the fact that Merkel cell carcinoma is a rare but highly invasive malignant cutaneous neuroendocrine carcinoma showing a high mortality rate of around 33%, which is even higher than that of melanoma.[3] Considering the worst case, age of 65 years or older adds up to a mortality rate of 30% regarding melanoma.[12] The harrowing statistics reflect an overall 5-year survival rate of MCC of 40%.[5] Unfortunately, physicians are still facing poor efficient therapeutic options.[3] Although, in terms of therapy a lot has been tried to fight effectively against MCC, such as radiation, chemotherapy, immunotherapy

and surgical excision, which is still the most important attempt next to recognition at an early stage.[2,13] Moreover, the incidence rates evaluated in Europe and the United States are on a steady rise.[9] During 1986 to 2001 a statistically significant annual increase of 8% had been detected in the United States.[14] An Australian study from Queensland revealed an annual overall increase of MCC incidence from 1993 to 2010 by an average of 2.6%. Youlden *et al*. highlighted that the incidence rates for MCC of 1.6 per 100.000 in Queensland are at least double those of any that have been previously published elsewhere in the world. The highest incidence rates were noted for persons 80 years or older (20.7 per 100.000). This fact is not surprising since Queensland presents a high-risk area due to a high ultraviolet (UV) light exposure of a predominantly Caucasian population who are quite keen on outdoor lifestyle.[8] Although, the impact of UV exposure is thought to play an immunosuppressive role rather than a mutagenic or carcinogenic one.[3,15] This fits perfectly to the predilection for the exposed and potentially chronically sun-damaged head and neck region of the skin where a tumor can be observed as a solitary firm-elastic to livid and rapidly growing nodule rapidly arising over weeks to months. Rarely also plaque-like variants are seen and thus more often on the trunk[2,3], which makes an early recognition crucial for a better overall outcome.[3]

Hence, risk factors for MCC involve age and immunosuppression. Patients who are under immunosuppression due to a history of organ transplantation or HIV infection have a higher risk for developing MCC; which occurs at a younger age.[2] Due to a tendency of an increase in life expectancy as well as an increase in immunocompromised patients, the steady rise in incidence rates of MCC seems not surprising at all.[13]

In virus-induced cancers, immune surveillance is employed in favor of tumor progression and survival. Prominent examples of viruses include the human papilloma virus, Epstein-Barr virus, human T-lymphotropic virus 1, Kaposi's sarcoma herpesvirus, and hepatitis B and C virus. [16] A similar effect could potentially play a role in MCC's tumorigenesis due to an important discovery related to viral infection of a previously completely unknown human virus.[17]
This breakthrough happened in 2008 with the identification of a 5387-base-pair genome of the previously unknown polyomavirus by Feng *et al*. in course of their search for viral sequences monoclonally integrated into the MCC tumor genome via

employing digital transcriptome subtraction analysis.[18] Moreover, it was shown that the viral integration occurs prior to clonal expansion of the MCC tumor cells.[19] Ultimately, this resulted in a better understanding of MCC pathogenesis. This group termed the unknown virus *Merkel cell polyomavirus* (MCPyV).[18] It is characterized as a small circular double-stranded deoxyribonucleic acid (DNA) virus, which encodes five to nine proteins, among them a tumor antigen(TAg) oncoprotein locus from an early region.[19,20] Furthermore, viral small T antigen (sTAg) as well as large T antigen (LTAg) are expressed in MCPyV-positive MCC cells, which are predicted to modulate both tumor suppressor and cell cycle regulatory proteins.[19,21] Moreover, in 80% viral DNA was detected to be integrated into MCC cells genome, corresponding 8 out of 10 MCC tumors.[18] This might present the basis for a potential mechanism to induce malignant transformation. Along this line it is worth noting that MCPyV-infection is quite common in humans but just a limited number of affected patients is going to develop MCC during lifetime.[22]

It has to be highlighted that MCPyV-encoded LTAg expression is required by infected MCC cells for their proliferation and survival since it has the ability to inactivate the tumor suppressor protein retinoblastoma protein Rb.[20,23] If by mutation of the conserved RB binding motif, the RB binding is impaired, MCC cells are in turn affected in their proliferation.[19] Interestingly, in a recent paper published by Kwun *et al*. the importance of the conserved LTAg phosphorylation sites was demonstrated via knock out of Fbw7, βTrCP, and Skp2 Skp-F-box-cullin (SCF) E3 ubiquitin ligases, which promotes MCPyV genome replication. These authors revealed that mutations at two of these phosphoreceptor sites, precisely at serine 220 and serine 239, increase LTAg levels and the MCPyV virion production and transmission. Moreover, they concluded that MCPyV reacts to stress stimuli such as nutritional starvation with the initiation of active viral transmission through SCF E3 ligase activities. Furthermore, this unique form of protein-mediated viral latency might be essential for a long-term or chronic viral perisistence, which after years could participate in the development of MCC.[24]

1.2 The tumor suppressor function of PTEN

Dysregulation of pathways that control major hallmarks of cell proliferation is common to all cancer entities. [25]

In general it can be stated mutational inactivation of tumor suppressor genes that would inhibit cancer development and oppose oncogene function, two genetic events are required to have an effect on both gene copies.[26,27] There is a variety of possibilities how the gene copies are lost or inactivated, e. g. chromosomal deletion or miss-segregation, epigenetic modifications known as epigenetic silencing such as methylation of a promoter region or overexpression of micro ribonucleic acids (RNAs) that target for example PTEN messenger RNA.[28,29,30,31,32] This aforementioned target leads to the tumor suppressor central to this master thesis, which is PTEN. As described in more detail below, the PTEN gene plays a key regulatory role in many types of advanced cancers if deleted or partially lost, which is well known for advanced tumors such as prostate, renal, small cell lung, endometrial, meningioma as well as melanoma.[32,33,34,35,36,37,38,39] Concerning an association between MCC tumorigenesis/tumor progression and a potential role of PTEN alterations and subsequent inactivation, evidence is scarce.

A literature search performed on the 12th of October 2017, using the terms "*PTEN and mutation*" in PubMed retrieves 4028 paper articles.[40] Moreover, by entering the search terms "*PTEN and loss*" retrieves 3149 publications.[41] This is an enormous body of literature regarding the topic of the tumor suppressor PTEN and it's critical role as a negative feedback regulator via it's lipid phosphatase activity in vital cellular functions and importantly as a major player in the phosphatidylinositol 3- kinase/v-akt murine thymoma viral oncogene homolog (PI3K/AKT) signaling pathway.[23,42] Surprisingly, by using the research terms "*PTEN and Merkel cell carcinoma*" PubMed links to four research papers.[43]

However, there is literature such as the work by Fernández-Figueras *et al*. who showed with their immunohistochemical studies of 31 MCC formalin-fixed tissue samples downregulation of PTEN in all stained tissue samples. Considerations regarding MCPyV-status were not involved in this study.[11] Those findings suggest to have a closer look on this prominent player and the pathway it's interacting regarding MCC

cells to reveal a potential inactivation thus, whether being a driver in tumorigenesis of MCC or not.

In 1997 Li *et al*. described for the first time a gene spanning 105 kb that includes nine exons located on human chromosome 10q23.31 encoding a 403-amino acid residue protein.[44,45] Moreover, it shows a protein tyrosine phosphatase domain which also exhibits a large region of homology of approximately 175 amino acids to chicken tensin and bovine auxilin, both classified as cytoskeletal proteins. Consequently, they named it *PTEN* for (phosphatidylinositol (3,4,5) -triphosphate [PtdIns (3,4,5) P_3]) Phosphatase and Tensin homolog deleted on chromosome Ten.[42,45,46] They hypothesized that if PTEN acts as a tumor suppressor that the PTEN allele with loss of heterozygosity (LOH) should exhibit inactivating mutations.[45]

PTEN is a pleiotropic protein with a dual-specificity, namely cytosolic lipid and tyrosine phosphatase activity.[47] As already mentioned, it is a major player in regulating a variety of cellular processes such as self-renewal and differentiation of human embryonic stem cells and hematopoietic stem cells, cell proliferation and apoptosis.[42,47] PTEN is crucial for proliferation, survival, differentiation and migration.[48] It also was found to regulate neutrophils chemotaxis. Many of crucial functions are determined by its lipid phosphatase activity, more precisely the N-terminal lipid-binding motif. The phosphatase encoded by the PTEN gene is able to dephosphorylate a lipid second messenger PtdIns (3,4,5) P_3 or PIP_3, which in turn is required for AKT activation. Thus, active PTEN inhibits PI3K signaling in the cytosol. In contrast a C-terminal tail phosphorylation is associated with a constraint state of PTEN in a closed conformation and to limit its association with the membrane and thus determines the resulting PtdIns (3,4,5) P_3 levels.[23,42,47] The survival kinase AKT1 is affected since PtdIns (3,4,5) P_3 induces downstream phosphorylation and thus AKT1 activation.[23] Moreover, altered AKT activity affects downstream targets such as fork head box protein O (FOXO), the E3 ubiquitin ligase mouse double minute 2 homolog (MDM2) and BCL2 antagonist of cell death (BAD; as illustrated in Fig. 1). In addition, PTEN antagonizes signaling cascades downstream of receptor tyrosine kinases (RTKs), well-known growth factor receptors, via the regulation of the cellular PtdIns (3,4,5) P_3 concentration.[23,42,47] Crucially, cells lacking PTEN phosphatase show elevated levels of PtdIns (3,4,5) P_3 and consequently active AKT (which is also known as protein kinase B).[49]

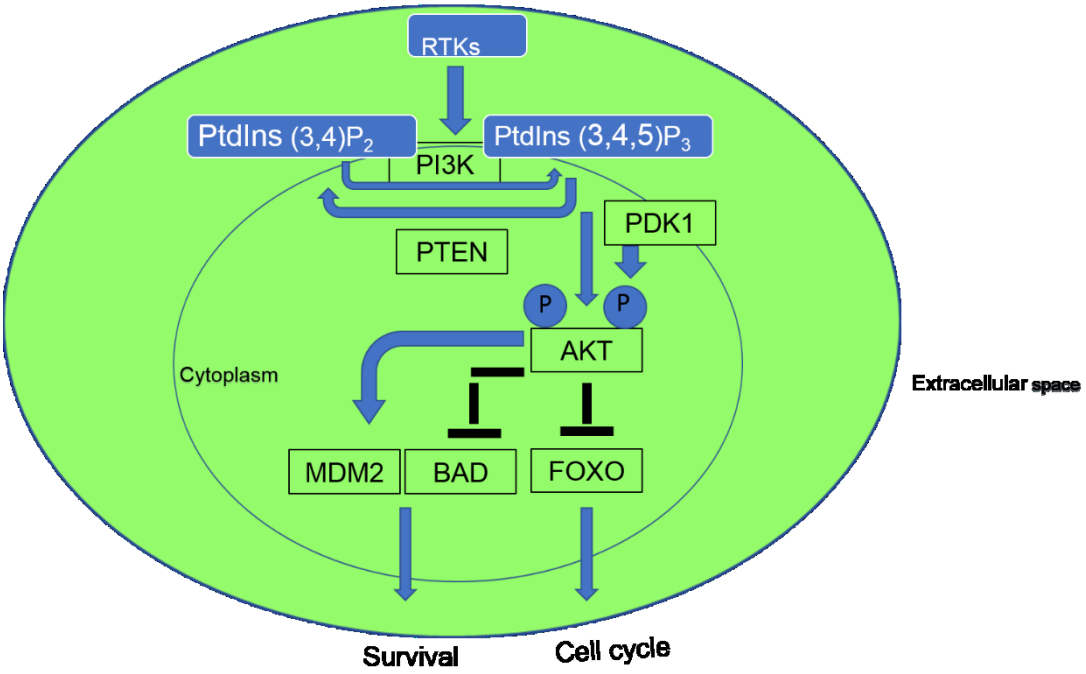

Fig. 1: Representation of PTEN as a prominent negative feedback regulator illustrated in a simplified model of the PI3K/AKT signaling pathway showing just a limited number of players and functions.

Subsequently PTEN was shown to be one among the most frequently mutated and deleted tumor suppressor genes in sporadic human cancers based on loss-of-function mutations affecting the phosphatase domain of PTEN.[31,46] Already in the early 1990's it was strongly suspected that alterations to the 10q22-25 region found in prostate, renal, small cell lung and endometrial carcinomas as well as melanoma and meningioma might be related to one or more tumor-suppressive loci.[32,33,34,35,36,37,38,39] Steck *et al.* verified homozygous deletions in a region at chromosome 10q23-24, and subsequently identified a gene, which they named MMAC1 for *mutated in multiple advanced cancers 1* which highlights its potential role in tumorigenesis of a variety of carcinomas.[45,50]

In MCC a heterozygous loss of an entire chromosome 10, where PTEN is located, precisely at 10q23.31, had been observed by Van Gele et al. in 21% of cases.[44,45,51] Therefore, it seems likely that aberrations in the PI3K/AKT pathway are causally connected with MCC pathogenesis[23], although, homozygous loss was only detected in case of one tumor out of 26 MCC tumor samples performed by Van Gele *et al*.[44,51]

Moreover, it is an interesting aspect, that loss of nuclear localization of PTEN and cancer progression are linked in certain tissues.[42,]

1.3 The Circadian Timing System

Circadian clocks are cell-autonomous and self-sustained oscillators, also referred to as molecular timekeepers or pacemakers, which organize cell functions in a 24-hour periodicity via transcriptional/translational auto-regulatory feedback loops at a molecular level.[52,53] This periodicity is emphasized by the origin of the word 'circadian' which is derived from a Latin phrase meaning 'about a day'. In most tissues, they operate at a single cell level; thus, each cell has an endogenous rhythm.[54] However, there are exemptions to this fixed periodicity; in rapidly proliferating tissues such as the epidermis and intestine where the cell cycle phase is not congruent with the circadian cycle periodicity. With these exceptions the cell cycle duration lasts approximately as long as the circadian cycle, about 24 hours in most tissues.[55]

The circadian clock has a great impact on a variety of biological and physiological processes such as metabolism, hormone release, immune activity, ageing, cell signaling, regulation of body temperature, chromatin landscapes, transcriptional state, sleep-wake cycles, learning and memory or most importantly cell proliferation.[54,56,57,58,59]

Hence, the circadian clock with its executing and active players, the central and peripheral clocks, is acting according to environmental cues. Thus, it can be retrained or reset by drastic shifts as in light-dark cycle, which are experienced during long-distance flights while crossing multiple time zones as for example from Reykjavik, Iceland, to Auckland, New Zealand.[60] The unfavorable consequences of this clock perturbations by shifts in light-dark cycle and the resulting uncoupling of central and peripheral clocks is called jet lag, which in case of a chronic status is related to a higher risk for many diseases such as atherosclerosis, cardiovascular disease, or cancer.[61,62,63]

Furthermore, the master clock orchestrates the activity of oscillators, namely hypothalamic suprachiasmatic nucleus cells (SCN cells) which are able to synchronize

circadian oscillators to environmental cues via input pathways and via circadian output pathways the subordinate clocks in peripheral tissues.[52,60]

The pineal gland releases melatonin, which regulates the sleep cycle. Darkness stimulates whereas light inhibits melatonin production. Light-sensitive nerve cells in the retina send this signal to the SCN, then daylight information is transmitted to the spinal cord and finally to the pineal gland where melatonin synthesis is shut down. In addition, peripheral cells do have the ability to reset their endogenous rhythm in response to stimuli as mentioned previously.[53]

Interestingly, the circadian clock may establish temporal windows in which certain cell cycle transitions are favored or suppressed; also known as circadian gating of the cell cycle.[64,65]

The link or importance of focusing on associations between the cell cycle and the circadian clock is not only vital to cell's survival or fate, it's simply important because of the phase shift between normal or non-transformed and malignant cells in a dyssynchronous manner regarding cell proliferation and metabolism. 'Phase' is described as a mathematical parameter in terms of circadian oscillation of a given process. Phase is defined as the time of the peak of a cosine wave using the time at which the light turns on as the reference time (circadian time 0).[66]

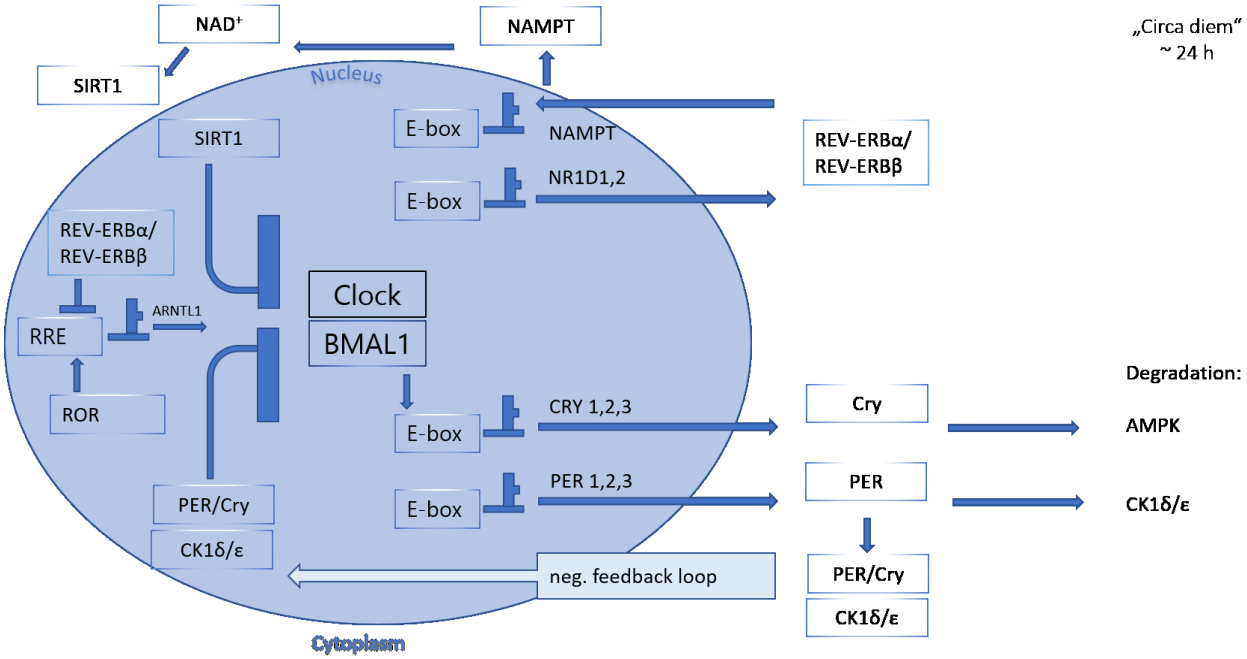

Fig. 2: A simplified model of the molecular circadian clock representing only the core negative feedback loop.

Fig. 2 presents a simplified model of the molecular circadian clock highlighting just the core regulatory negative feedback loop or pathway although it has to be mentioned that there are many positive and negative oscillators involved. The regulation of those master transcription factors occurs via transcriptional/translational negative feedback loops.[60]

The central circadian transcription factor CLOCK (circadian locomotor output cycles kaput) heterodimerizes in a complex with BMAL1 (brain and muscle, ARNT-like) that binds to E-box DNA elements present in the promoters of cryptochrome (CRY) and period (PER). This process leads to transcriptional activation of CRY and PER. An activation of transcription of most of the core clock genes such as CRY and PER, reverse erythroblastosis virus (REV-ERB) α and retinoic acid-related orphan receptor (ROR) clock genes occurs as a result at the beginning of a circadian day.[60] Cry and Per heterodimers suppress the activity of the BMAL1/CLOCK complex, while ROR and REV-ERB are able to promote or repress BMAL1 transcription.

CRY and PER, which are members of the most prominent negative pathway or feedback loop of the molecular circadian clock, which will be discussed in more detail.

Due to the ability of their protein products to form a complex together with casein kinase1 δ/ε (CK1δ/ε) in the cytoplasm at the end of a circadian day and because of their translocation into the nucleus, where the Cry protein dissociates from the complex to repress the activation of BMAL1/CLOCK-mediated transcription through direct protein-protein interactions, which in turn sets up the oscillations of CRY, PER and clock controlled genes (CCGs). If the process of complex-formation of the proteins CRY and PER together with CK1 δ/ε is impaired, they are destined for degradation. This is accomplished in case of the unbound CRY protein by phosphorylation via AMP-kinase (AMPK) and the single PER protein is phosphorylated by CK1 δ/ε in order to be degraded.[60] The impact of those and other players of the molecular circadian clock on the cell cycle will be discussed below.

1.4 Interactions between the Cell Cycle and the Molecular Circadian Clock and its implications

An overview of the eukaryotic cell cycle is displayed in Fig. 3. Cell division is a process that needs tight controls to enable normal cell division and accurate duplication of DNA in the chromosomes. The resulting two daughter cells contain chromosomes identical to those of the parental cell. DNA duplication occurs during S phase (S for synthesis), which is one of the two major molecular processes during the cell cycle. Chromosome segregation and cell division is part of the M-phase (M for mitosis). Resting intervals are in between these molecular processes: The first gap phase G1 between the M phase and S phase, is necessary for the cells to grow in size and synthesize RNAs and proteins required for DNA synthesis. Another gap phase G2 is between S phase and mitosis. [67]

Each individual event or step of the cell cycle has to be accomplished successfully to avoid malfunctions leading to inaccurate cell division or excessive cell divisions resulting in cancer. This is ensured by certain checkpoint pathways or regulatory proteins that govern the progression through the cell cycle. Alterations or inactivating mutations of these regulatory proteins contribute to cancer development. Master regulators are protein kinases, which inherit a catalytic subunit, the cyclin-dependent kinases (CDKs). In association with a regulatory cyclin subunit their kinase activity can be activated. The activity of CDKs is regulated by activators (cyclins) or inhibitors (INK,

Cip, or Kip proteins). Through phosphorylation of literally hundreds of proteins at specific regulatory sites, the cyclin-CDK complexes are able to work as activators or inhibitors. They are involved in the activation or inhibition of proteins, which are entering the cell cycle, acting in DNA damage, replication and mitosis. At specific checkpoints, the cell cycle can be arrested if previous events have not been completed successfully. Moreover, regulated degradation of proteins is also an important part of control. Furthermore, repair mechanisms can be activated if necessary. [67]

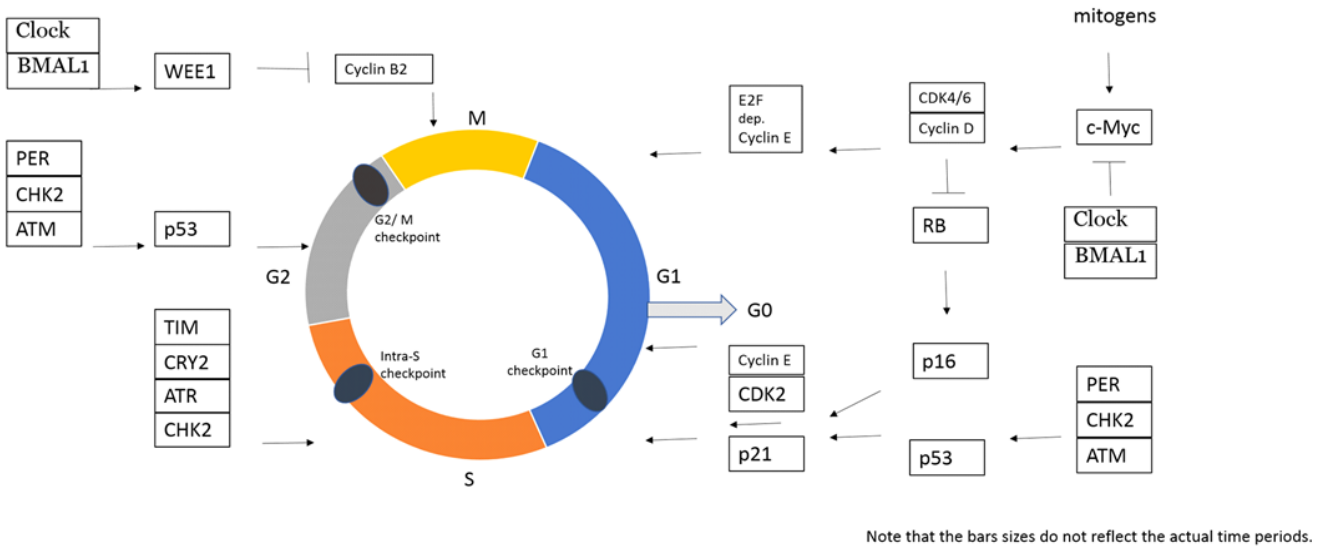

Fig. 3: Schematic representation of the Cell Cycle and the Molecular Circadian Clock.

Figure 3 gives an overview of players of the circadian timing system acting in the cell cycle. As outlined, extracellular mitogen signals have to be present to transiently activate early genes. Due to its complexity, the focus is just on specific pathways and interacting partners. As an example, myelocytomatosis viral oncogene homolog c-Myc induces Cyclin D and subsequently activates Cyclin D/cyclin-dependent kinase CDK4/6 complex thus activating E2F-dependent Cyclin E expression by suppressing tumor suppressor RB. Moreover, the interaction of Cyclin E with CDK2 allows the transition of gap (G) 1 to synthesis (S) phase.[63]

Activation of c-Myc or E2F triggered by excessive DNA damage or uncontrolled oncogenic signaling would lead to an elevated cyclin expression. Thus, G1 checkpoint

activation is inhibited by the tumor suppressor protein p16 and p21 which are under control of RB and p53, respectively. So, the cyclin complexes are disrupted and the cells are set for a dividing break by entering G0.[63] In early G1 the BMAL1/Clock heterodimer complex downregulates Myc transcription in order to prevent an overexpression. In the G2 regulators interact with the checkpoint kinase ataxia telangiectasia mutated (ATM)/checkpoint kinase (CHK) 2 and induce p53 signaling as a reaction to DNA double strand breaks. BMAL1/Clock plays an additional role in preventing mitotic (M) phase entry via Wee1 activation if necessary.[63]

1.5 How does PTEN fit into the concept of the molecular timekeepers?

Considering the fact that many members of the clock gene family are upregulated, and thus the molecular circadian rhythm is dysregulated in tumor cells as described by Matsuomoto *et al.* [68], it is highly unlikely that the prominent key regulator PTEN presents itself as an exemption. Indeed, Zhang *et al.* demonstrated that PTEN is acting (in accordance to its tumor suppressive function) as a regulator in hematopoietic stem cell (HSC) quiescence.[48] The ability of the circadian clock to maintain homeostasis of mammalian physiology at molecular, cellular, tissue and organismal level enables its tumor suppressive function. Accordingly, Zhang *et al*. observed that downregulation of PTEN in human epithelial cells by employing small interfering ribonucleic acid (siRNA) technology led to nuclear accumulation of BMAL1 as well as elevated levels of $pAKT^{Ser473}$.[48] PTEN therefore could affect the function of core clock players, which are shown in Fig. 3.

It has been shown that non-transformed or normal cells and malignant cells are significantly different in terms of metabolism and proliferation.[63] These aberrations can be determined since the circadian gene expression rhythm is acting in a fixed phase relationship with the timing of cell division. Thus, circadian genes might be altered in cancer cells in order to outcompete non-transformed cells, which are slowed down by having rest phase every 24 hours.[55,63] This special way of employing and manipulating the proliferative machinery of the very own host cell could be specifically turned against the MCPyV for targeted therapy in accordance to chronotherapeutic schemata.

For my own thesis the fact that PTEN as well as Clock are proteins which are able to shuttle between the nucleus and cytoplasm to carry out distinct functions, required a technique to feasibly separate nuclei from the cytosol of MCC cells.[47,69]

2 Objective

The role of PTEN loss in many cancer entities is clearly demonstrated.[32,33,34,35,36,37,38,39] However, in MCC, an entity with relatively small incidence rates the role of PTEN loss/activity during tumor progression/metastasis is less clear.

To start preparatory work in MCC I pursued two aims during my master thesis, namely

i) to clarify whether MCPyV expression determines expression levels of PTEN and activation/phosphorylation of AKT

and

ii) characterize the subcellular localization of PTEN and evaluate colocalization with CLOCK.

3 Materials and Methods

MCC cell lines and Cell culture. The MCC 13 MCPyV-negative adherent cell line was established in the Queensland Radium Institute Laboratory (Queensland Institute of Medical Research, Brisbane, Queensland, Australia) from a metastatic cervical node obtained from an 80-year-old female patient.[17,23,51,70,71,72]

MCC 26 is an adherent MCC cell line and MCPyV-negative, which was established from the recurrence of a tumor in an 82-year-old female patient at the Queensland Radium Institute Laboratory. MCC was confirmed by a biopsy of the lesion at the left lateral calf.[71,72]

The University of Michigan UM-MCC 623.39 MCPyV-negative adherent and spheroidal MCC cell line was derived from human tumor xenografts in NOD/SCID/IL2rγ^{null} mice of a primary tumor located at the arm of a 54-year-old male patient.[21,73,74,75] The NSG mice were established at the Jackson Laboratory, Bar Harbor, ME).[21] NSG is an abbreviation for non-obese diabetic (NOD)/severe combined immune deficient (SCID) mice, homozygous for the mutation Prkdcscid, thus a null mutation in the interleukin-2 common gamma chain receptor (IL2rγ^{null}).[75,76]

Another MCPyV-negative spheroidal MCC cell line is UM-MCC 34, which was derived from a metastatic axillary lymph node of a male patient at the age of 88 years at diagnosis.[21]

The MCPyV-positive MCC single cell line suspension WaGa was derived from ascites of a 67-year-old male MCC patient of the Department of Dermatology, Venereology and Allergology, University Hospital Würzburg (Würzburg, Germany) or established at the Department for Translational Dermato-Oncology (DKTK), University Hospital Essen (Essen, Germany) as stated by Paulson *et al*..[17,23,72,77]

From nodal metastasis of a 26-year-old male MCC patient the MCPyV-positive MKL-1 single cell suspension cell line was established by the original creator Masahiro Shuda at the University of Pittsburgh Cancer Institute, University of Pittsburgh, (Pittsburgh, United States of America).[17,20,23,72,77]

The MCPyV-positive single cell suspension cell line MKL-2 was established from a 72-year-old Caucasian male at the Robert H. Lurie Comprehensive Cancer Center at the Northwestern University, (Chicago, Illinois, United States of America).[17,72,78,]

In addition, the single cell suspension cell line PeTa harbors viral DNA, which was established at the Department of Dermatology, Venereology and Allergology, University Hospital Würzburg (Würzburg, Germany).[72]

The single cell suspension cell line AsTi is MCPyV-positive as well; unfortunately, no further descriptive data was available.

Another single cell suspension MCPyV-positive cell line established at the Department of Dermatology, Venereology and Allergology, University Hospital Würzburg (Würzburg, Germany) is WoWe 2; further descriptive data was not obtained.[72]

The MCPyV-positive adherent and spheroidal cell line UKE-MCC 4a was established at the University Medical Center Hamburg Eppendorf (UKE); no further descriptive data could be verified.
MCC metastasis located at the leg of a female 54-year-old patient is the source for the MCPyV-positive MCC single cell suspension cell line UM-MCC 13, established at the University of Michigan.[21]

MS-1 is a MCPyV-positive single cell suspension MCC cell line derived from an adrenal metastasis of a 59-year-old female patient at the Department of Dermatology, Venereology and Allergology, University Hospital Würzburg (Würzburg, Germany).[17]

Cell culture. All cell lines were maintained in RPMI-1640 medium supplemented with 10% fetal calf serum (FCS) as well as 1% P/S (100 U/ml penicillin and 0.1 mg/ml streptomycin).

Trypsinisation of cells. Cells were washed with 1x PBS (w/o without magnesium and calcium). Trypsinisation performed by pre-warmed T/E via a water bath at 37°C, containing 0.05% trypsin as well as 0.02% EDTA.

Cell count. Vital cell number was determined by counting cells excluding undiluted 1:1 trypan blue dye in 4 times 4 squares of a Neubauer chamber. The mean value out of three determinations was used to calculate via simple final account cells needed for $7*10^6$ cells per ml for each experimental set-up sample either heat-shock treated or not. Cells were washed in phosphate buffer saline (PBS; without calcium and magnesium).

Heat-shock treatment. Cells were incubated at 42°C for 30 minutes on a thermo shaker (PHMT Grant-bio; 24*1.5 ml attachment) in order to establish circadian synchronization. Afterwards, incubated at 37°C over-night with 5% CO_2-level.

Lysate preparation; including Buffer Solutions for Nuclear and Cytosolic Extractions as well as for Whole Protein Extractions.

Preparation of stock solutions.

Table 1: First, the stock solutions were prepared as follows; adjusted to 50 ml or 2 ml with Aqua dist., respectively.

Reagent	**Volume**	**Concentration**	**Molecular weight**	**Weighed in**
DTT	2 ml	0.1 M	154.3 g/mol	0.3086 g
HEPES pH 7.5	50 ml	0.5 M	238.3 g/mol	5.95 g
KCl	50 ml	1 M	74.56 g/mol	3.7 g
NaCl	50 ml	2 M	58.44 g/mol	5.8 g
Nonidet-40 (Igepal)	50 ml	10 %		

Preparation of protein extraction (PE) buffer: To 10 ml of RIPA buffer (Radio Immuno Precipitation buffer), 100 µl of 1 M NaF, 100 µl of 100 mM PMSF were added as well as one cOmplete™ Mini tablet containing protease inhibitors.

Preparation of cytoplasmic extraction (CE) buffer; stored at 4° Celsius (C) for a maximum of two weeks). To obtain 10 ml of CE buffer 200 µl of 0.5 M HEPES pH 7.5 stock solution were used as well as 100 µl of 1 M KCl stock solution, 2 µl of 0.5 M EDTA, 100 µl of 100 mM DTT, 50 µl of PMSF (0.1 M in ethanol) and 1 cOmplete™ Mini tablet were added together with 9.548 ml of aqua (H_2O) dist. to get to a final

concentration of 10 mM HEPES pH 7.5, 10 mM KCl, 0.1 mM EDTA, 1 mM DTT and 0.5 mM PMSF.

Preparation of nuclear extraction (NE) buffer; stored at 4°C for a maximum of two weeks). For a final NEB buffer volume of 10 ml 400 µl of 0.5 M HEPES pH 7.5 stock solution, 2 ml of 2M NaCl stock solution, 20 µl of 0.5 M EDTA, 100 µl of 100 mM DTT, 100 µl of PMS (0.1 M in ethanol), as well as 1 cOmplete™ Mini tablet and 7.380 ml of aqua dist.; to obtain a final concentration of 20 mM HEPES pH 7.5, 400 mM NaCl, 1 mM EDTA, 1 mM DTT and 1mM PMSF.

To separate nuclei from cytoplasmic fractions, 9 µl of 10% Igepal (Nonidet-P40) were carefully added to each sample to obtain a final concentration of 0.257%.

Determination of protein concentration. The protein concentrations were determined by the bicinchoninic acid (BCA) method; Pierce™ BCA Protein Assay Kit obtained from Thermo Fisher Scientific. For the standards 10 µl of bovine serum albumin/Albumin Fraction V (BSA) 2 mg/ml, a 1:1 dilution (25 µl of BSA and 25 µl H_2O dist., correspondingly), a 1:5 dilutions (10 µl of BSA; 40 µl of H_2O dist.), a 1:10 dilution (5 µl BSA; 45 µl of H_2O dist.) were used. BSA was from ROTH.

Gel preparation and sample loading. Either whole cell lysates or nuclear and cytosolic protein fractions were separated by sodium dodecyl sulfate-polyacrylamide gel electrophoresis (SDS-PAGE; 10%) for 100 minutes at 90 Volt; afterwards blotted to a nitrocellulose membrane. Whereupon, the lower gel solution (10%) for one gel was prepared by the addition of 2900 µl of acrylamid-bis (19:1, 30% w/v), 2170 µl of lower gel buffer, 3530 µl of aqua dist. and 86 µl SDS-solution of 10%. Afterwards, 4.36 µl of TEMED and 76.00 µl of APS were added under the flow hood. For the preparation of upper gel solution (3.9%) 326 µl of acrylamid-bis (19:1, 30% w/v), 500 µl of upper gel buffer, 1650 µl of glycerin 50% and 21.5 µl SDS-solution (10%) were needed. Additionally, 1.25 µl of TEMED and 19 µl of APS (10%) were added under the flow hood as well.
The transfer was performed for 95 minutes at 150 Milliampere. Regarding the Western blot loading, 25 µg of distinct extracted protein were loaded per lane as well as 4 µl of protein ladder (Page Ruler; 10 to 180 kDa).

Preparation of 1x SDS Running buffer. The 1x SDS Running buffer was prepared by adding 100 ml of 10x SDS Running buffer (containing 30.3 g Tris, 150.1 g glycine, 10 g SDS) to 1 l of H_2O dist.

Preparation of 10x Blotting buffer. In order to prepare 10x Blotting buffer, 12.1 g of Tris as well as 30 g of glycine are weighed in 1 l bottle and filled up with 1000 ml of Aqua dist.; the buffer was mixed on a rotating plate.

Preparation of 1x Blotting buffer. For the preparation of 500 ml of 1x Blotting buffer 50 ml of 10x Blotting buffer (ice-cold stored at 4ºC) and 100 ml of methanol (under the hood) were added to 350 ml of aqua dist. and mixed on a rotating plate; stored at 4°C.

Preparation of fat-free milk powder 5% in 1x Washing buffer (TBS and Tween) by weighing in 10 g of fat-free milk powder, filled up to 200 ml with 1x Washing buffer; pH was adjusted to 7.4 via the help of a pH-meter and by using 1 M NaOH and 32% HCl, correspondingly.

Primary and secondary antibodies. The membranes, tightly sealed in a plastic foil, were incubated with either 4 µl of anti-PTEN antibody (1:1000; rabbit monoclonal antibody mAb; #9559 obtained from Cell signaling) in 4 ml of 5% BSA in TBST; 4 µl of anti-pAKT^{S473} antibody (1:1000; rabbit; #9271 obtained from Cell signaling) in 4 ml of 5% BSA in TBST; 4 µl of anti-AKT antibody (1:1000; rabbit;#9272 obtained from Cell signaling) in 4 ml of 5% BSA in TBST; 2 µl of anti-β-Tubulin (1:2000; mouse mAb; #T4026 obtained from Sigma Aldrich) in 4 ml of 5% fat-free milk in 1x Washing buffer (TBST; pH 7.4). Moreover, the primary antibodies employed for nuclear and cytoplasmic extraction, 4 µl of anti-CLOCK antibody, monoclonal rabbit (1:1000; #5157 obtained from Cell signaling) in 4 ml of 5% BSA in TBST; 4 µl of anti-β-Actin (1:1000; rabbit mAb #4970 obtained from Cell signaling) in 4 ml of 5% BSA in TBST and 4 µl of anti-Lamin B1 antibody (1:1000; rabbit polyclonal Ab; #16048 obtained from Abcam; Cambridge, United Kingdom) in 4 ml of 5% BSA in TBST.

Each membrane was incubated with the adequate secondary antibody, polyclonal goat anti- rabbit secondary antibody conjugated with horseradish peroxidase (HRP) (0.25 g/l; #P0448 obtained from DAKO) in case if a primary rabbit antibody was used. To 10 ml of 5% fat-free milk in 1x Washing buffer (TBST; pH 7.4) 3.33 µl of the polyclonal goat anti-rabbit HRP antibody were added and mixed gently in order to obtain a 1:3000

dilution. In contrary, if a primary mouse antibody was employed the membrane was incubated with the adequate secondary antibody, polyclonal rabbit anti-mouse conjugated with HRP (1.3 g/l; #P0260 obtained from DAKO) as in case of anti-β-Tubulin. To 10 ml of 5% milk in 1x Washing buffer (TBST; pH 7.4) 3.33 µl were added and mixed gently in order to obtain a 1:3000 dilution.

Preparation of 10x Washing buffer. In order to prepare 1 l of 10x Washing buffer 90 g NaCl and 12.1 g of Tris were weighed in a glass beaker, 5 ml of Tween were added under the hood and filled up to 400 ml of aqua dist.. The buffer was thoroughly mixed on a rotating platform. Then the pH was adjusted to 7.4 via the help of a pH-meter. Afterwards it was filled up to 1000 ml with aqua dist.. Again, the buffer was mixed on a rotating platform and the pH was once more adjusted to a pH of 7.4 via adding 1 M NaOH and 32% HCl, respectively.

Signal development. Each membrane, with the exemption of the membrane incubated with anti-pAKT^{S473} antibody, was covered with 500 µl of Pierce^{TM} EC Western Blotting Substrate, which had been prepared as follows. 250 µl of peroxide solution detection reagent 1 was mixed with 250 µl of luminol enhancer detection reagent 2. Just the membrane incubated with anti-pAKT^{S473} antibody was visualized by covering it with 500 µl of Super Signal West Femto solution, which had been prepared as follows. 250 µl of reagent A were mixed with 250 µl of reagent B. Visualization was performed by employing Amersham Imager 600 where the manual function had been used.

Table 2: Detailed listing of all employed primary and secondary antibodies, their predicted band sizes for WB, species origin, supplier, ordering number and storage conditions.

Antibodies	Molecular weight (kDa)	Species origin	Supplier	Order No.	Storage
Primary Ab.					
• anti-AKT	60-(62)	rabbit	Cell signalling	9272	-26°C or 4° in 5% BSA+TBST (1:1000)
• anti-pAKT^{S473}	60-65	rabbit	Cell signalling	9271	-26°C or 4° in 5% BSA+TBST (1:1000)
• anti-β-Actin	45	rabbit mAb. (IgG isotype)	Cell signalling	4970S	-26°C or 4° in 5% BSA+TBST (1:1000)

• anti-PTEN	55	rabbit mAb.	Cell signalling	9559	-26°C or 4° in 5% BSA+TBST (1:1000)
• anti-Lamin B1	66-70	rabbit polyclonal Ab.	Abcam	16048	-26°C or 4° in 5% BSA+TBST (1:10000)
• anti-β-Tubulin	55	mouse mAb. (IgG1 isotype)	Sigma Aldrich	T4026	-26°C or 4° in milk+TBST (1:2000)
• anti-CLOCK	120	rabbit mAb. (IgG isotype)	Cell signalling	5157	-26°C or 4° in 5% BSA+TBST (1:1000)
Secondary Ab.					
• polyclonal goat anti-rabbit HRP (0.25 g/l)		rabbit polyclonal Ab. (IgG isotype)	Dako	P0448	4° in 5% milk+TBST (1:3000)
• polyclonal rabbit anti-mouse HRP (1.3 g/l)		mouse polyclonal Ab. (IgG isotype	Dako	P0260	4° in 5% milk+TBST (1:3000)

Table 3: Listing of the chemicals used in the experimental processing with detailed data about molecular weight, supplier, ordering number and storage conditions.

Chemicals	Abbreviation	Molecular weight	Supplier	Order No.	Storage
Acrylamid/Bis Solution 30% (w/v) (19:1)			Bio-Rad Laboratories GmbH	161-0154	RT
Ammonium persulfate	APS	228.20 g/mol	Bio-Rad Laboratories GmbH	1610700	RT (powder)/ -26°C, 10% aliquots (500 µl)
Aqua distilled	H_2O		Self-provided		On use.
Bovine serum albumin/ Albumin Fraction V > 98%; 2mg/ml	BSA		ROTH		RT powder (stock); aliquot at 4° C
1-Butanol (< 0.5% water)		74.12 g/mol	Carl Roth GmbH	7724.1	RT (safety locker, liquid)
cOmplete™, Mini Protease Inhibitor Cocktail			Sigma Aldrich	11836153001	4°C (tablet)

Dithiothreitol	DTT	154.3 g/mol	Bio-Rad Laboratories GmbH	161-0610	4°C (powder)/ -26°C, 100 mM aliquots (500 µl)
Dulbecco`s Phosphate - phosphate buffer saline (w/o (without) $Ca^{2+,}$ $Mg^{2+)}$	DPBS		PAN-Biotech GmbH	P04-36500	RT 4°C (15 ml aliquots)
Ethylenediaminetetra-acetic acid	EDTA	372.24 g/mol	ThermoFisher Scientific or BioRad	15575-038	RT (powder)/ RT liquid stock 0.5 M
Fetal calf serum 10%	FCS		Biochrom GmbH (M)		-26° C
Glycin	Gly/G	75.0666 g/mol	Bio-Rad Laboratories GmbH	161-0718	RT (powder)
Glycerin			Carl Roth GmbH	3783.2	
Hydrogen chloride 32%	HCl				RT
4-(2-hydroxyethyl) -1-piperazineethanesulfonic acid	HEPES	238.3 g/mol			RT (powder)/ liquid stock 0.5 M pH 7.5
5x loading buffer (containing β-mercaptoethanol)					-26°C aliquots
β-Mercaptoethanol > 99%			Carl Roth GmbH	4427.3	RT
Non-fat dried milk powder			AppliChem GmbH	A0830	RT (powder)/ 4°C liquid stock 5% pH 7.4
Nonited-P40 substitute (Igepal)			US Biologicals	HM2076	RT (liquid)/ RT stock 10%
Page Ruler™ (pre-stained protein ladder 10 to 180 kDa)			ThermoFisher Scientific	26616	-26°C
1% of Penicillin (100 units/ml) and Streptomycin (0.1 mg/ml); Stock of 10.000 U/ml penicillin and 0.1 mg/ml streptomycin	P/S		PAN BIOTECH		-26°C
Phenylmethanesulfonyl fluoride (0.1 M in ethanol)	PMSF	760.57 g/mol	Sigma Aldrich	93482	4°C (liquid)
Ponceau S red			Sigma Aldrich	P3504	RT (liquid, under the hood)

Potassium chloride	KCl	74.56 g/mol	Carl Roth GmbH	2312118	RT (powder)/ RT liquid stock 1 M
RIPA buffer	RIPA		Sigma Aldrich	R0278	4°C (liquid)
RPMI-1640 medium (supplemented with 10% fetal calf serum & 1% P/S (100 U/ml penicillin; 0.1 mg/ml streptomycin)	RPMI		PanTech		4°C (liquid)
Sodium chloride	NaCl	58.44 g/mol	Sigma Aldrich	31434	RT (powder)/ RT liquid stock 2 M
Sodium dodecyl sulfate	SDS		Carl Roth GmbH	4360.2	RT (powder)
Sodium fluoride 1 M	NaF	41.99 g/mol	Sigma		RT (powder)/ -26°C, 100 µl aliquots 1 M)
Sodium hydroxide 1M	NaOH				RT
Tetramethylethylen-diamine	TEMED	116.21 g/mol	AppliChem GmbH	A1148	4°C (liquid)
Tris(hydroxymethyl)-aminomethan	Tris	121.14 g/mol	Carl Roth GmbH	0188.2	RT (liquid stock 1 M pH 8.0)

Table 4: Kit systems used in the course of the experiment, including a description of reagents, supplier, ordering number and storage conditions.

Trade Name	**Contains**	**Supplier**	**Order No.**	**Storage**
Pierce™ BCA Protein Assay Kit	BCA reagent A & B	Thermo Fisher Scientific	23225	RT
Pierce™ EC Western Blotting Substrate	Peroxide solution detection reagent 1 (1.125 ml) Luminol Enhancer detection reagent 2 (2.125 ml)	Thermo Fisher Scientific	32209 (Product No.)	4°C
Super Signal™ West Femto Maximum Sensitivity Substrate	Reagent A & B	Thermo Fisher Scientific	34094	4°C

Table 5: List of technical equipment used during experiments.

Technical description/ Trade name	**Supplier & Notes**
Amersham Imager 600	
BIO RAD WB equipment BIO-RAD Supply, Mini PROTEAN® Tetra System and BIO-RAD POWER PACTM Basic (as well as stands, glass plates (short plates and spacer plates with 1.5 mm, combs (10 or 15 well; 1.5 mm), plastic roller, sponges, transfer-filter paper (thicker ones obtained from BIO-RAD; Mini Trans-Blot®; 7.5x10 cm/ thinner ones obtained from Biozym Scientific GmbH; 8x10 cm); nitrocellulose membranes	BIO-RAD
Centrifuge	Universal 320R (cooling possible)
Centrifuge (Megafuge)	Heraeus Megafuge 16 R; max 5000 rpm (cooling possible)
Flurostar Omega	
Incubator	
Microscope & Neubauer chamber	
Rotating platform	Rotating shake genie
Sealing advice polystar 245	
Suction extractor unit	Integra Vacusip
Thermo shaker	PHMT Grant-bio; 24* 1.5 ml attachment
Vortexer	
Water bath Phoenix WB12	Phoenix WB12

3.1. In-depth description of Methods

3.1.1 Western blotting

After the preparation of the distinct cellular extracts, a method needs to be employed in order to identify the protein of interest accurately in a sample of a variety of proteins.

Western blot or blotting is such a particular detection technique to identify distinct proteins; in contrast to Southern blot or Northern blot, where specifically DNA or RNA is detected, correspondingly.

First, the sample of proteins is denatured. This step is performed by using heat, a reducing agent and sodium dodecyl sulfate (SDS).[84]

Due to the specific properties of proteins, which are polymeric molecules it is possible to separate them electrophoretically by size.[84,85] With the help of the anionic detergent SDS, which binds to approximately every two amino acids, the proteins become polyanions. Importantly, the number of negative charges is directly proportional to the size or molecular weight of the protein destined for detection. If an electric field is applied, the protein in turn will subsequently migrate towards the anode due to its negative charges.[85]

Additionally, Western blotting is also referred to as immunoblotting since the protein can only be detected if an antibody specific to the protein of interest is available. By the way, this antibody is called primary antibody, such as a rabbit antibody. This is possible since a completed gel electrophoretogram can be blotted onto a sheet of nitrocellulose or polyvinylidene difluoride (PVDF), which in turn binds the blotted proteins nonspecifically. In order to block excess adsorption sites on the nitrocellulose, which is used in this particular experimental set-up; and thus, to prevent nonspecific adsorption of an antibody, the milk protein casein is applied.

After the removal of the unbound primary antibody by a washing step, the membranes are incubated with a secondary antibody, such as an enzyme-linked goat anti-rabbit antibody.[86] The covalently linked enzyme is horseradish peroxidase (HRP), which is necessary for specific detection of the protein of interest. Then, again, a washing step is performed to remove the unbound secondary antibody. In the following, the enzyme in the bound secondary antibody can be assayed via a colorimetric reaction.

Whereupon, bands appearing on the nitrocellulose membrane can be identified as the protein of interest.[86]

Furthermore, via immunoblot analysis it can be evaluated whether the protein of interest is upregulated, downregulated, cleaved, phosphorylated, glycosylated or ubiquitinated.[87]

3.1.2 Whole cell/protein lysis of 13 MCC cell lines destined for the expression verification regarding PTEN via employing Western blotting

Cell culture

All previously described thirteen cell lines were maintained as described in the section *Cell culture* of chapter 3 *Materials and Methods*.

Trypsinisation of cells

Old media, namely RPMI-1640 supplemented with 10% FCS as well as 1% P/S (100 U/ml penicillin and streptomycin 0.1 mg/ml), of each adherent cell line such as MCC 13 and MCC 26 as listed in table 6, are discarded by aspiration under the flow bench. Except for the cell lines appearing as adherent cells as well as spheroids, namely UM-MCC 623.39 and UKE-MCC 4a; the old media containing the spheroids are transferred into distinct 50 ml falcon tubes. The cells are washed once with 3 ml of 1x PBS (w/o without magnesium and calcium). Afterwards, 3 ml of mildly preheated T/E via a water bath at 37°C, containing 0.05% trypsin as well as 0.02% EDTA, are transferred to each cell sample and the cell clusters are re-suspended. The cells are incubated for 3 min at 37°C with 5% CO_2 level in a cell culture incubator. In the following, the cells are detached by chipping the culture flask. If a successful detachment can be observed under the microscope, 8 ml of RPMI-1640 medium supplemented with 10% FCS as well as 1% of P/S are added to each cell line and carefully aspirated three times. Subsequently, the cell solutions are transferred into distinct 50 ml falcon tubes each.

Lysis of whole cells/proteins

PE buffer is prepared as listed in the previous section *Preparation of protein extraction (PE) buffer* of chapter 3 *Materials and Methods*.

The cell line samples as listed in table 6 are centrifuged at 300 g (Heraeus Megafuge 16 R) for 5 min at room temperature (RT), the supernatants are discarded. In the following, the cells are washed once with 1 ml of ice-cold PBS (w/o calcium and magnesium), which has to be placed on ice in advance. Moreover, the samples are centrifuged at 3000 rpm for 8 min at 4°C (Universal 320R). The supernatants are discarded. To each pellet 60 µl of PE buffer are added, thoroughly re-suspended and transferred into distinct 1.5 ml Eppendorf tubes. The samples are incubated on ice for 15 min.. Afterwards centrifuged at 14.000 rpm for 10 min at 4ºC (Universal 320R). Each supernatant is transferred into a distinct 1.5 ml Eppendorf tube.

Determination of protein concentration using BCA Protein Assay kit

First, the amount of BCA working reagent has to be calculated (BSA; 1:50). Since each of the thirteen samples, a blank (H_2O) and the four standards are pipetted into two distinct wells each (thus twice) and in order to have a back-up for two additional samples, BCA working reagent is prepared for 38 samples. Into each sample per well 196 µl of BCA reagent A and 4 µl of BCA reagent B are pipetted. Therefore, a stock containing 7448 µl reagent A and 152 µl of reagent B is prepared. For the standards 10 µl of BSA 2 mg/ml, a 1:1 dilution (25 µl of BSA and 25 µl H_2O dist., respectively), a 1:5 dilution (10 µl of BSA; 40 µl of H_2O dist.), a 1:10 dilution (5 µl BSA; 45 µl of H_2O dist.) are pipetted into two distinct wells each. The samples are diluted 1:5 (4 µl of sample; 16 µl of H_2O dist.). To each well of a microplate 10 µl of each distinct sample (twice each) prepared as described above are pipetted as well as 200 µl of BCA working reagent. The prepared microplate is gently shaken and incubated for 30 min at 37ºC in an incubator before the measurement with Flurostar Omega can be performed. The values of obtained absorbance are noted and evaluated; calculation according to a standardized formula is executed to obtain the actual concentration of each sample. The volume of 5x loading buffer to be added can be calculated with the help of a standardized calculation formula. Then to each sample the calculated volume of 5x loading dye is added. Additionally, they are boiled for 5 min at 95ºC on a thermo shaker (PHMT Grant-bio; 24* 1.5 ml attachment) and afterwards stored at -20ºC. If the obtained concentration of the samples is sufficient, the samples can be split into several aliquots to prevent repeated thawing.

Gel preparation

Preparation of lower gel solution (10%) for one gel is performed as described in section *Gel preparation and sample loading* of chapter 3 *Materials and Methods*.

The glass plates (1.5 mm) are cleaned and checked for cuts. BIO-RAD stands and clips are used. Subsequently, after preparation of the gel, it is poured into the space between the two glass plates. In order to get rid of potential bubbles in the gel a butanol layer is applied of approximately 200 µl. Then the gel is set for polymerization for about 30 minutes. Afterwards, the butanol is washed away by using H_2O dist.. Detailed description of the preparation of upper gel solution is listed in section *Gel preparation and sample loading* of chapter 3 *Materials and Methods*.

Subsequently, the solution is poured on top of the lower gel solution and a comb (15 well, 1.5 mm) is inserted. Again, the gel is set for polymerization for about 30 minutes. After polymerization, the gel is wrapped in water-saturated tissue papers and stored at 4ºC in a plastic bag if not processed further.

Loading as well as running of the gels

Potentially left smear is removed from the gels, which had been prepared previously. Moreover, the comb is removed carefully. In the following, each gel is placed into the tank together with an empty plastic plate on the opposing site as well as an additional empty stand. The right placement regarding anode and cathode has to be followed. A marking on the front side of the glass plate is set to enable an easier loading as well as to prevent pipetting errors. Afterwards, the tank is filled up to the black mark of the tank with 1x SDS running buffer. Each well is washed with the help of a syringe with running buffer contained in the tank. It is noted to keep the wells straight. Regarding the Western blot, 25 µg of extracted protein are loaded per well of each 10% SDS-Page gel as shown in table 6 as well as 4 µl of protein ladder (Page Ruler; 10 to 180 kDa). Prior to loading, each sample is shortly vortexed and spun down. The gels are run for approximately 100 minutes at 90 Volt. Whereupon, it is taken care that the loading dye is not exceeding the green mark of the tank.

Table 6: The loading scheme of each sample as well as protein ladder of the experimental set-up regarding PTEN expression, to be loaded on a 10% SDS-Page gel in order to load 25 µg of extracted protein as well as further information about the cell lines employed.

Lane (from left to right)	2	3	4	5	6	7	8	9	10	11	12	13	14	15
Sample	Protein Ladder (Page Ruler; 10 to 180 kDa)	**MCC 13**	**MCC 26**	**UM-MCC 623.39**	**UM-MCC 34**	**WaGa**	**MKL 1**	**MKL 2**	**PeTa**	**AsTi**	**Wo We 2**	**UKE-MCC 4a**	**UM-MCC 13**	**MS1**
Virus status		**- MCPyV-neg.**	**-**	**-**	**-**	**+ MCPyV-pos.**	**+**	**+**	**+**	**+**	**+**	**+**	**+**	**+**
		adherent	**adherent**	**adherent; spheroides**	**spheroides**							**adherent; spheroides**		

Transfer of the protein from the gel to the membrane

The nitrocellulose membrane is incubated for 5 minutes in 1x Blotting buffer, even before the stacking had been started yet. The fixating plates are placed into a bigger tray filled with 1x Blotting buffer to be completely saturated. A sponge is placed on each plate on top of them together with a filter paper each. The nitrocellulose membrane is placed on top of the filter paper of the anode side. On top of this half sandwich, the gel is placed gently. In order to remove bubbles, a gently rolling technique is applied by using a small plastic comb, which is gently rolled under the filter paper and over the gel. After placing the stacked sandwich into the tank together with an ice pack, which has been stored at -20ºC, the tank is filled up to the black mark with ice-cold 1x Blotting buffer with the intention to reduce the heat generated during the blotting process. The transfer is performed for 95 minutes at 150 Milliampere (mA). In the following, the

membranes are stained with Ponceau S Red for about 30 secs. before the blocking step will be performed. Subsequently, the membranes are washed with aqua dist.. The membrane is cut as tight as possible to avoid waste of applied antibody. It is cut at around 35 kDa into an upper and a lower piece of membrane.

Antibody staining

Then the upper and lower membrane pieces are blocked for about 2 hours at RT by using 5% fat-free milk powder in 1 x Washing buffer (TBST; pH 7.4) on a rotating platform at 14 rpm in two distinct petri dishes. Moreover, they are incubated separately over night at a rotating platform at level 1.7 at 4ºC in a plastic foil sealed previously twice (next to the already sealed location; during the sealing process, the foil is additionally wrapped in aluminum foil for a better sealing outcome) for 5 secs. at level 3 via a plastic foil sealer, polystar 245. Each plastic foil package containing antibodies with either 4 µl of anti-AKT (1:1000; rabbit; #9272 obtained from Cell signaling) in 4 ml of 5% BSA in TBST; 4 µl of anti-pAKT^{S473} (1:1000; rabbit; #9271 obtained from Cell signaling) in 4 ml of 5% BSA in TBST; 2 µl of β-Tubulin (1:2000; mouse mAb; #T4026 obtained from Sigma Aldrich) in 4 ml of 5% fat-free milk powder in TBST (pH 7.4) or 4 µl of PTEN (1:1000; rabbit mAb; #9559 obtained from Cell signaling) in 4 ml of 5% BSA in TBST. In case of re-staining the membrane, it has to be washed three times with 1x Washing buffer prior to incubation with the antibody. On the following day, the membranes are washed with 1x Washing buffer and incubated on a rotating platform at 70 rpm for 10 minutes at RT. This washing step is performed three times in total.

Then the membranes are incubated with the adequate secondary antibody. Polyclonal goat anti-rabbit secondary antibodies conjugated with horseradish peroxidase (HRP) (0.25 g/l; #P0448 obtained from DAKO) in case of anti-AKT, anti-pAKT^{S473} and anti-PTEN incubated membranes; just for the membrane incubated with anti-β-Tubulin the secondary antibody has to be polyclonal rabbit anti-mouse conjugated with HRP (1.3 g/l; P0260 obtained from DAKO). To 10 ml of 5% fat-free milk (in TBST; pH 7.4) 3.33 µl of the polyclonal goat anti-rabbit HRP antibody are added and mixed gently in order to obtain a 1:3000 dilution. Thereafter, 10 ml are poured onto the membranes each, incubated with anti-AKT, anti-pAKT ^{S473} and anti-PTEN. Concerning the membrane incubated with anti- β-Tubulin 3.33 µl of polyclonal rabbit anti-mouse HRP are poured together with 10 ml of 5% fat-free milk powder in TBST (pH 7.4) onto this membrane.

Therefore, to each membrane, 10 ml of the appropriate secondary antibody-milk solution are transferred.

The membranes are incubated at 4°C for two hours at level 1.7 on a rotating platform. Thereafter, the membranes are washed with 1x Washing buffer for at least one hour at RT on a rotating platform at 70 rpm. In addition, every 20 minutes (five times in total, 1 hr. 40 min) the 1x Washing buffer has to be exchanged for a new one.

Signal development

Signal development was performed via placing the membrane on a plastic foil and thus by covering it with 500 µl of Pierce™ EC Western Blotting Substrate, which is exactly prepared as described in section *Signal development* of chapter 3 *Materials and Methods*. The membranes are incubated for three minutes. Then the membranes are visualized via using Amersham Imager 600, the manual function is used. The exposure period should be chosen specifically according to the obtained outcome. For -20°C storage, the membranes need to be sealed via using the plastic foil sealer polystar 245; level 3 is used and pressed for 5 seconds (sealed twice; next to the already sealed location; during the sealing process, the foil is additionally wrapped in aluminum foil for a better sealing outcome).

3.1.3 Nuclear and cytosolic protein fractionation

A reliable technique to study dynamic changes in intracellular protein localization is termed as nuclear and cytosolic/cytoplasmic subcellular fractionation of proteins. The earliest steps in the progress of developing a successful fractionation of cell components were achieved by Warburg in 1913 by means of centrifugation.[79] Nowadays, most protocols are further developments based on the protocol established by Dignam *et al*. in 1983.[80,81]

First, the cells of interest, of course MCC cells in this case, have to be harvested; whereupon the adherent and spheroid cell lines are harvested by trypsinization before sequential lysis of plasma and nuclear membrane can be performed. In the following, the cells are re-suspended in hypotonic lysis buffer to swell up the cells in order that the cell walls will burst. Importantly, the nuclear membrane will be kept intact during the first steps. Moreover, this lysis buffer is not containing any detergent.[82] Afterwards; the

plasma membrane of the swollen cells is lysed by adding non-ionic, non-denaturing detergent since it is important to keep the extracted proteins in their native form. In this experimental set-up, each sample is incubated on ice with the detergent Nonited-P40 substitute Igepal for the purpose to separate the nuclei from the cytoplasmic fractions. Then the nuclei are pelleted and the supernatants representing the cytoplasmic fractions are collected.[82] In the following, the nuclear proteins can be extracted by using nuclear extraction (NE) buffer with the intention to burst the nuclear membranes. Another centrifugation step is performed. Whereupon, the obtained pellets are reflecting only cell membrane debris. The obtained supernatants are in contrast representing the final nuclear fractions.

In order to verify the efficiency of the fractionation process specific antibodies targeted against the protein of interest are employed by Western blotting, which will be discussed in the section *Western blotting*.[83]

Cell culture

The WaGa cell line was maintained in RPMI-1640 medium supplemented with 10% fetal calf serum (FCS) as well as 1% P/S (100 U/ml penicillin and 0.1 mg/ml streptomycin).

Cell count

A falcon tube containing WaGa cells (approximately 25 ml; split previously), cultured as described in the previous section *Cell culture*, is taken out of the incubator (37°C; 5% CO_2). In order to count the cells under the microscope, 20 µl of trypan blue (undiluted, 1:1) are mixed with 20 µl of the WaGa cell sample. 10 µl of this mixture are pipetted to the Neubauer chamber; 4*4 squares are counted twice for vital cells. The mean is taken and multiplied by 2 (as a dilution factor) times 10^4. The volume of culture medium containing the WaGa cells needed for $7*10^6$ cells/ml is calculated via simple final account. It has to be noted that for the experimental set-up dyssynchronous control cells, two distinct 50 ml tissue culture flasks are necessary since cells are destined for either nuclear and cytosolic extraction or whole protein lysis as well; each containing $7*10^6$ cells/ml. In the following, those dyssynchronous control samples (volumes depending on cell count result) are transferred into a 50-ml culture flask each and filled

up to 15 ml with RPMI-1640 medium supplemented with 10% fetal calf serum as well as 1% P/S (100 U/ml penicillin; 0,1 mg/ml streptomycin) in order to obtain about 1:3.6 dilution. In the following incubated at 37°C with 5% CO_2 level for approximately 24 hours until further processing.

Heat shock (HS) treatment

Afterwards, the two samples (volumes depending on cell count result) are transferred into distinct 1.5 ml Eppendorf tubes each (for HS nuclear/cytoplasmic (N/C) and whole protein lysis (WP)), destined to be incubated at 42°C for 30 minutes on a thermo shaker. Afterwards, the samples entrained by heat shock are transferred into a distinct 50 ml culture flask each (one for HS N/C and one for WP) and filled up to 15 ml with RPMI-1640 medium supplemented with 10% fetal calf serum as well as 1% P/S (100 U/ml penicillin; 0.1 mg/ml streptomycin) in order to obtain about 1:3.6 dilution. The culture flasks are then incubated at 37°C with 5% CO_2 level for approximately 24 hours.

Nuclear and cytosolic fractionation

All non-whole cell/protein extraction samples (2*) as well as the whole cell/protein lysis samples are centrifuged at 1500 rpm (Heraeus Megafuge 16 R) for 5 min at RT, the supernatants are removed via a suction extractor unit (Integra Vacusip). The whole cell/protein samples are in the meanwhile kept on ice until further processing. The cells are washed once with 1 ml of ice-cold PBS (w/o magnesium and calcium), which has to be placed on ice in advance. Another centrifugation step is performed at 1500 rpm (Heraeus Megafuge 16 R) for 5 min at RT followed with subsequent removal of the supernatants according to the previous description. Each cell pellet is carefully re-suspended in 350 µl of cytoplasmic extraction (CE) buffer, aspirated thoroughly, and transferred into a 1.5 ml Eppendorf tube each, which are subsequently incubated on ice for 15 min. It has to be noted that the tubes are going to be flicked every 5 min. Then, 9 µl of 10% Nonidet-P40 (Igepal) are carefully added to each sample, which are again incubated on ice for 15 min, every 5 min flicking is performed. The samples are centrifuged at 3000 rpm for 8 min at 4ºC (Universal 320R), the acceleration is set and brake is on 1. The supernatants, which reflect the cytosolic fractions (either heat-shocked or dyssynchronous/untreated), are transferred into new 1.5 ml Eppendorf tubes each. Thereby, the transferred volumes are noted carefully. The remaining pellets are washed twice in 200 µl ice-cold PBS each with subsequent centrifugation at

3000 rpm for 8 min at 4ºC, acceleration is set as well as brake on 1. Afterwards, the supernatants are discarded. To each pellet 50 µl nuclear extraction (NE) buffer are added, and the samples are carefully re-suspended. The samples are vortexed for at least 15 min at 4ºC by using a special attachment fixture on top of the vortexer at level 7. The samples are centrifuged at 14.000 rpm for 10 min at 4ºC (Universal 320R). 50 µl of nucleus supernatant are transferred into a new Eppendorf tube each, to reflect the final nuclear fractions, which are subsequently stored together with the cytosolic fractions at -20ºC if not further processed.

Lysis of whole cells/proteins of either heat-shock treated or dyssynchronous/untreated samples

The two whole cell/protein extraction samples are centrifuged at 1500 rpm (Heraeus Megafuge 16 R) for 5 min at 4°C, the supernatants are discarded. Further processing of the samples is performed as described in section *Lysis of whole cells/proteins* of chapter *3.1.2 Whole cell/protein lysis of 13 MCC cell lines destined for the expression verification regarding PTEN via employing Western blotting*. The tubes are subsequently stored at -20ºC if not further processed by employing BCA assay amongst other subsequent handling.

Determination of protein concentration via using BCA Protein Assay kit

First, the amount of BCA working reagent has to be calculated (BSA; 1:50). Since each of the six samples, a blank (H_2O) and the four standards are pipetted each into two wells (twice) and in order to have a back-up for two additional samples, BCA working reagent is prepared for 24 samples. Into each sample per well 196 µl of BCA reagent A and 4 µl of BCA reagent B are pipetted. Therefore, a stock containing 4707 µl reagent A and 96 µl of reagent B is prepared. The standards are prepared as described in section *Determination of protein concentration using BCA Protein Assay kit* of chapter 3.1.2 *Whole cell/protein lysis of 13 MCC cell lines destined for the expression verification regarding PTEN via Western blotting*. In addition, the further processing is performed exactly according to this description.

Gel preparation

The gels are prepared accordingly as described in the section *Gel preparation* of the chapter 3.1.2 *Whole cell/protein lysis of 13 MCC cell lines destined for the expression*

verification regarding PTEN employing Western blotting. It just has to be mentioned that a 10 well comb of 1.5 mm is used instead of a 15 well comb.

Loading as well as running of the gel

The preparations prior to loading the gel are performed exactly as described in section *Loading as well as running of the gels* of chapter 3.1.2 *Whole cell/protein lysis of 13 MCC cell lines destined for the expression verification regarding PTEN employing Western blotting*. The wells are loaded as shown in table 7, whereby the amount of extracted protein for loading is decided upon the obtained protein concentrations. As for example 25 µg per well. The gel is run for 100 minutes at 90 V. Whereupon, it is taken care that the loading dye is not exceeding the green mark of the tank.

Table 7: The loading scheme of each sample as well as protein ladder of the experimental set-up nuclear and cytoplasmic extraction as well as total cell lysates of heat-shock treated and untreated/ desynchronized WaGa samples, to be loaded on a 10% SDS-Page gel in order to load 25 µg of extracted protein. Note that the loading scheme regarding this experimental set-up had been changed once.

Lane (from left to right)	2	3	4	5	6	7	8
Sample	Protein Ladder (10 to 180 kDa Page Ruler)	Total lysate HS (WaGa)	Total lysate non-HS (WaGa)	NE HS (WaGa)	NE non-HS (WaGa)	CE HS (WaGa)	CE non-HS (WaGa)

Transfer of the protein from the gel to the membrane

The transfer of the protein from the gel to the nitrocellulose membrane is performed according to the description in section *Transfer of the protein from the gel to the membrane* of the chapter 3.1.2 *Whole cell/protein lysis of 13 MCC cell lines destined for the expression verification regarding PTEN employing Western blotting.*

Antibody staining

Then, the membranes are blocked for about 90 minutes at RT by using 5% fat-free milk powder in 1x Washing buffer (pH 7.4) on a rotating platform at 14 rpm in distinct petri dishes. Moreover, incubated separately over night at the rotating platform at level 1.7 at 4ºC in a plastic foil sealed previously twice (next to the already sealed location; during

the sealing process, the foil is additionally wrapped in aluminum foil for a better sealing outcome) for 5 sec. at level 3 via a plastic foil sealer, polystar 245. Each plastic foil package containing antibodies with either 4 µl of anti-β-Actin (1:1000; rabbit mAb; #4970 obtained from Cell signaling) in 4 ml of 5% BSA in TBST; 4 µl of anti-PTEN (1:1000; rabbit mAb; #9559 obtained from Cell signaling) in 4 ml of 5% BSA in TBST; 0.4 µl of anti-Lamin B1 antibody (1:10000; rabbit polyclonal Ab; #16048 obtained from abcam; Cambridge, United Kingdom) in 4 ml of 5% BSA in TBST; 2 µl of β-Tubulin (1:2000; mouse mAb; #T4026 obtained from Sigma Aldrich) in 4 ml of 5% fat-free milk powder in TBST (pH 7.4) or 4 µl of anti-CLOCK antibody, monoclonal rabbit (1:1000; rabbit mAb; #5157 obtained from Cell signaling) in 5% BSA in TBST. In case of re-staining the membrane, it has to be washed three times with 1x Washing buffer prior to incubation with the antibody. On the following day, the membranes are washed with 1x Washing buffer and incubated on a rotating platform at 70 rpm for 10 minutes at RT. This washing step is performed three times in total. Then the membranes are incubated with the adequate secondary antibody, polyclonal goat anti-rabbit conjugated with horseradish peroxidase (HRP) (0.25 g/l; #P0448 obtained from DAKO) as follows. To 10 ml of 5% fat-free milk powder in TBST (pH 7.4) 3.33 µl of the antibody are added and mixed gently in order to obtain a 1:3000 dilution. In the following, to each membrane, 10 ml of secondary antibody-milk solution are transferred. Just in case of the membrane incubated with anti-β-Tubulin the secondary antibody has to be polyclonal rabbit anti-mouse conjugated with HRP (1.3 g/l; P0260 obtained from DAKO). Concerning this membrane 3.33 µl of polyclonal rabbit anti-mouse HRP are poured together with 10 ml of 5% fat-free milk in TBST (pH 7.4) onto this membrane. Therefore, to each membrane, 10 ml of the appropriate secondary antibody-milk solution are transferred. The membranes are incubated at RT for 2 hrs. at 14 rpm on a rotating platform. Thereafter, the membranes are washed with 1x Washing buffer for at least one hour at RT on a rotating platform at 70 rpm. In addition, every 20 minutes (five times in total, 1 hr. 40 min) the 1x Washing buffer has to be exchanged for a new one.

Signal development

Signal development was performed exactly as described in section *Signal development* of chapter 3.1.2 *Whole cell/protein lysis of 13 MCC cell lines destined for the expression verification regarding PTEN employing Western blotting.*

4 Results

4.1 PTEN expression by MCPyV- and MCPyV+ MCC cell lines

To get an indication whether the presence of MCPyV determines PTEN expression in MCC cells of different origin, whole cell lysates were analyzed by Western blotting. As can be seen in Fig. 4A PTEN, pAKT^{S473}, total AKT, and β-Tubulin (used as loading control) were detected at the expected molecular masses of 55, 65, 62, and 55 kDa, respectively. PTEN was detectable in all cell lines and expression appears to be unaffected by the MCPyV status. pAKT levels were highly variable between the different cell lines and highest expression was observed in MCC26 and UM-MCC13 cells. In contrast, total AKT expression was relatively stable in all cell lines investigated (Fig. 4A).

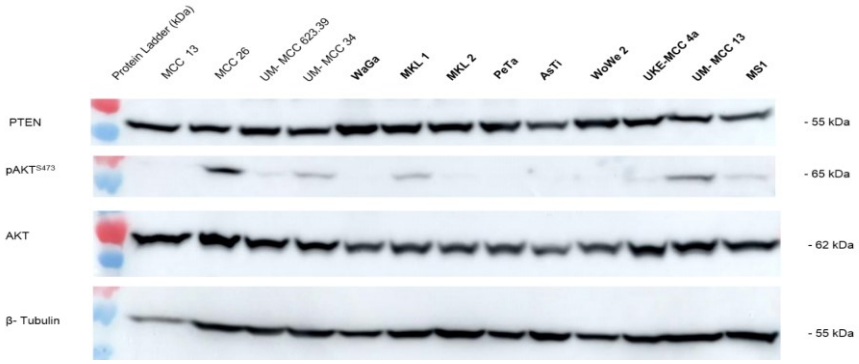

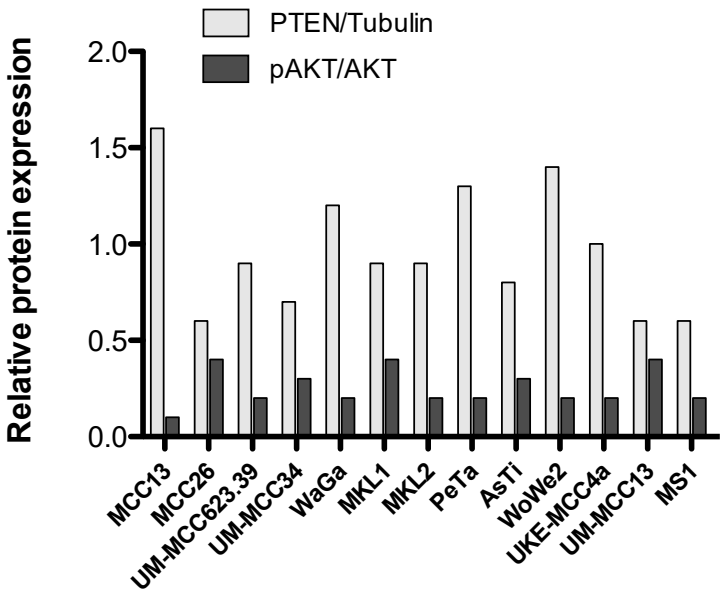

Fig. 4: A.) PTEN, pAKT^{S473}, AKT and β-Tubulin expression in four MCPyV-negative and nine MCPyV-positive (in bold letters) MCC cell lines of total cell lysates, detected by Western blotting (15 well gel; 25 µg of extracted protein loaded/well of a 10% SDS-PAGE gel with exposure times of 50 sec. for PTEN, 15 min. for pAKT^{S473}, 4 min. for AKT and 50 sec. for β-Tubulin). It has to be noted that these blots were spliced together.

B.) Relative protein expression where PTEN was normalized to β-Tubulin and pAKT ^{S473} to total AKT signals.

In Fig. 4B shown PTEN and pAKT levels normalized to β-Tubulin and total AKT, respectively. From these normalized data, it is obvious that PTEN expression in the different MCC cell lines differs approximately threefold.

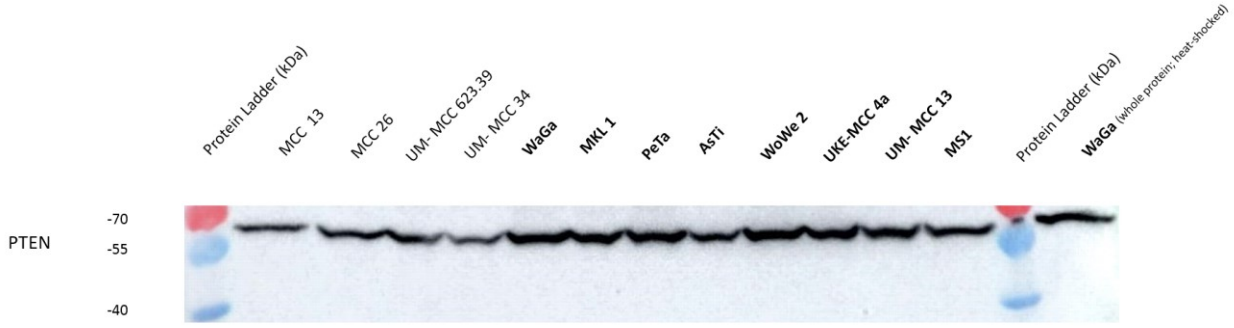

Fig. 5: PTEN expression in four MCPyV-negative and eight MCPyV-positive MCC cell lines (in bold letters) and an additional heat-shock treated WaGa sample of total cell lysates, detected by Western blotting (15 well gel; 25 µg of extracted protein loaded/well of a 10% SDS-PAGE gel with an exposure time of 5 sec.).

To get first indications whether heat shock treatment of cells alters PTEN signals I have treated WaGa cells at 42°C for 30 min prior to analysis (last lane in Fig. 5). However, from this experiment it appears that the PTEN signal is not heat shock-sensitive.

4.2 Analysis of CLOCK expression in the nuclear and cytosolic compartment of WaGa cells

In a first set of experiments WaGa cells were cultured under standard conditions or subjected to heat shock, followed by subcellular fractionation (to obtain nuclei and the remaining cytosolic fraction) and Western blot analysis. From a different set of culture dishes (absence or presence of heat shock), total protein extracts were obtained. As can be seen from Fig. 6 CLOCK was detected as a double band at 120 and 90 kDa respectively, which is in line with data shown in the Santa Cruz data sheet. Of note, CLOCK was exclusively detected in the nuclear compartment with no immunoreactive signal obtained with the cytosolic samples. As observed for PTEN, CLOCK Western blot signals from cells cultured under standard conditions or subjected to heat shock did not differ substantially (Fig. 6).

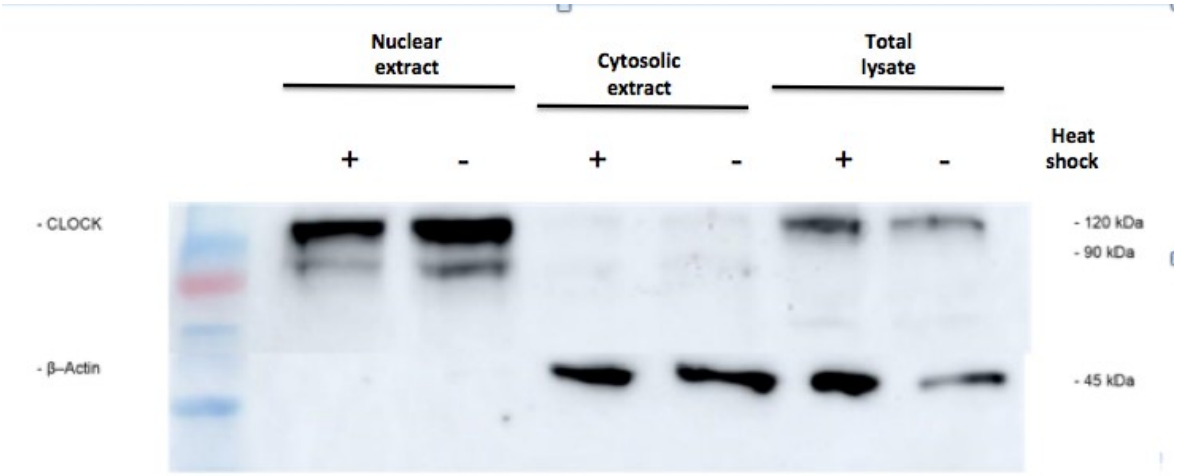

Fig. 6: CLOCK and β-Actin expression of the experimental set-up nuclear and cytosolic fractionation in MCPyV-positive MCC cell line WaGa either heat-shock treated for 30 min. at 42°C or desynchronized as well as total cell lysates detected by Western blotting (10 well gel; 25 µg of extracted protein loaded/well of a 10% SDS-PAGE gel with exposure time of 4 sec.). These blots were spliced together. NE = nuclear extract, CE = cytosolic extract, PE = total protein extract, HS = heat shock.

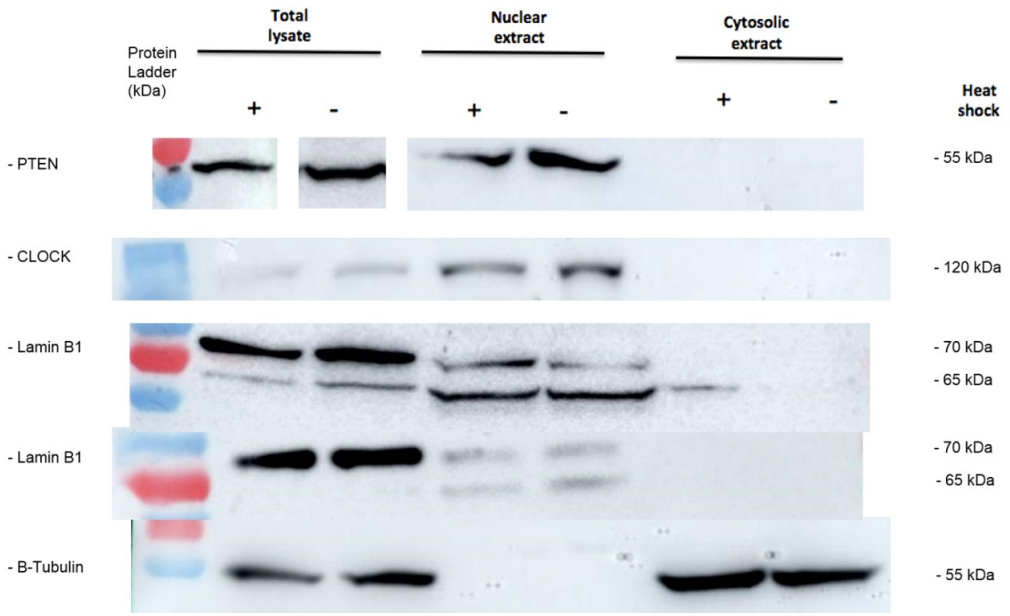

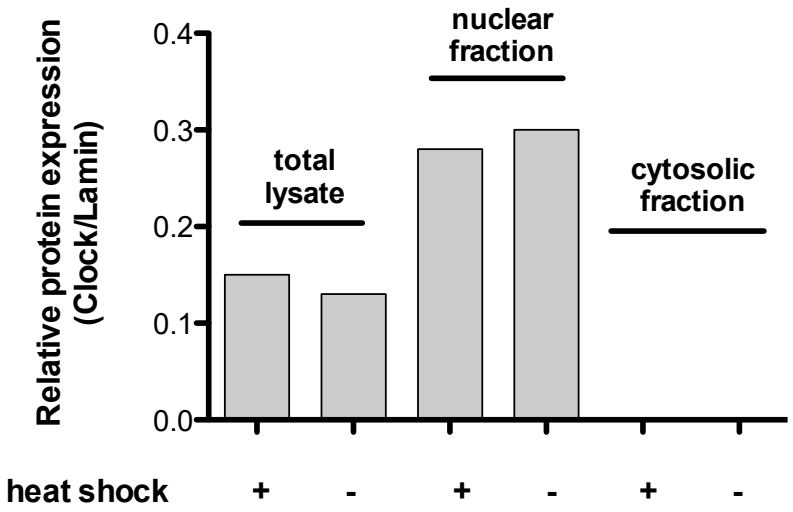

Fig. 7: A.) PTEN, CLOCK, Lamin B1 and β-Tubulin expression of the experimental set-up nuclear and cytosolic fractionation in MCPyV-positive MCC cell line WaGa either heat-shock treated for 30 min. at 42°C or desynchronized as well as total cell lysates demonstrated via Western blot (10 well gel; 25 µg of extracted protein loaded/well of a 10% SDS-PAGE gel with exposure times of 5 sec. for the total cell lysate PTEN samples, 1 min. for the nuclear and cytosolic PTEN samples, 4 sec. for CLOCK, 5 sec. for the upper Lamin B1 samples, 50 sec. for the lower Lamin B1 samples and 50 sec. for β-Tubulin). It has to be noted that these blots were spliced together. NE = nuclear extract, CE = cytosolic extract, PE = total protein extract, HS = heat shock.

B.) Relative protein expression where CLOCK was normalized to Lamin B1 signals.

In a second experiment I have included the analysis of PTEN and Lamin B1 (a nuclear marker) in my Western blot experiments (Fig. 7). These analyses revealed that PTEN is detectable only in nuclear compartment to an extent similar as observed for CLOCK expression. Again, heat shocked cells did show relatively little difference in signal intensities as compared to standard culture conditions (Fig. 7).

5 Discussion

5.1 The overall experimental design

The first aim of the present study was to reveal the expression of PTEN in MCPyV positive and -negative cell lines. As discussed in the chapter *The tumor suppressor function of PTEN*, alterations of PTEN and the subsequent function loss as an important driver in the progression of many cancers, have been demonstrated thoroughly.[32,33,34,35,36,37,38,39] In order to study PTEN protein expression in different MCC cell lines Western blotting was employed for four MCPyV-negative cell lines, which are termed MCC 13, MCC 26, UM-MCC 623.39 and UM-MCC 34, as well as nine MCC cell lines which harbor viral DNA. Those MCPyV-positive cell lines employed are WaGa, MKL1, MKL 2, PeTa, AsTi, WoWe 2, UKE-MCC 4a, UM-MCC 13 and MS-1. Immunoblotting was conducted by using anti-PTEN (rabbit mAb; #9559 obtained from Cell signaling) and anti-pAKT^{S473} (rabbit; #9271 obtained from Cell signaling) as well as anti-AKT (rabbit; #9272 obtained from Cell signaling) antibodies.

PTEN is an opposing player of AKT and this is of importance in cancer: One signal that is over activated in many cancer entities is the production of phosphatidylinositol (3,4,5) trisphosphate, a phospholipid that activates AKT on one hand and is degraded by PTEN on the other hand. Thus, it is clear that PTEN controls AKT activation by regulating the levels of available PIP_3 in the plasma membrane. As such, the phosphorylation status (‘activation’) of AKT would indirectly reflect the activity of PTEN and vice versa.[42,47] Thus, general remarks about an activation or inhibition of the PI3K/AKT pathway and its consequences could be deduced. In addition to the antibody directed against AKT phosphorylated at S^{473}, another antibody, which detects an activating phosphorylation site on AKT phosphorylated namely T^{308} could have been considered but due to availability options, just anti-pAKT^{S473} was employed. The total expression or protein level of AKT in comparison to the phosphorylated AKT is required to make valid statements about the activation status of AKT. Thus, phosphorylation at S^{473} reveals in a reliable manner possible activation of the protein, which cannot be due to changes in the dephosphorylated AKT.

As a loading control, also referred to as housekeeping protein, anti-β-Tubulin (mouse mAb; #T4026 obtained from Sigma Aldrich) is part of the experimental set-up.[89] Due to

the fact that MCPyV-positive as well as MCPyV-negative cell lines are tested, a potential expression difference might present itself to give a hint on underlying mechanisms of the MCPyV to outcompete non-transformed cells and thus to employ the cell's own proliferation machinery. Most importantly, whether integration of the viral DNA into the genome makes a significant difference in improved outcome or aggressiveness of this particular carcinoma and in the following might offer a possible target for future therapeutic treatments.

In the second part of my experimental set-up, MCPyV-positive WaGa cells were used. This cell line grows as single cell suspension making it a convenient culture model that is readily available. First, discrimination between synchronized and desynchronized WaGa cells is established. Synchronization of the cells is important since the synchronized state reflects the influence of the cell cycle on the circadian cycle. It is known that cells maintain their individual circadian rhythmicity in tissue culture. However, due to stochastic perturbations the cell culture as a whole does not display a homogenous circadian rhythm. Therefore, unless synchronized by extracellular signals or stimuli the entire cell culture is not exhibiting a common circadian rhythm.[90] For the purpose of cell cycle synchronization; the cells are starved for at least fourteen hours or a day. To establish circadian synchronization, the cells are entrained by a heat-shock treatment for 30 minutes at 42°C using a thermocycler for constant heat conditions. Subsequently, the cells are transferred into culturing flasks, incubated for 24 hours at 37°C and 5% CO_2. Amongst all designed set-ups, there is always a control cell sample, which is not subjected to any treatment; thus desynchronized. In total, I used three distinct experimental set-ups, including two samples each as illustrated in Fig. 8. Moreover, each sample is containing $7*10^6$ cells/ml, destined for either nuclear and cytoplasmic extraction or whole cell/protein lysis. It has to be noted that due to the ambitious experimental design, cell cycle synchronization was not part of the actual experiment. The focus of the present thesis was clearly on getting familiar with the experimental techniques and laying a starting foundation for future studies.

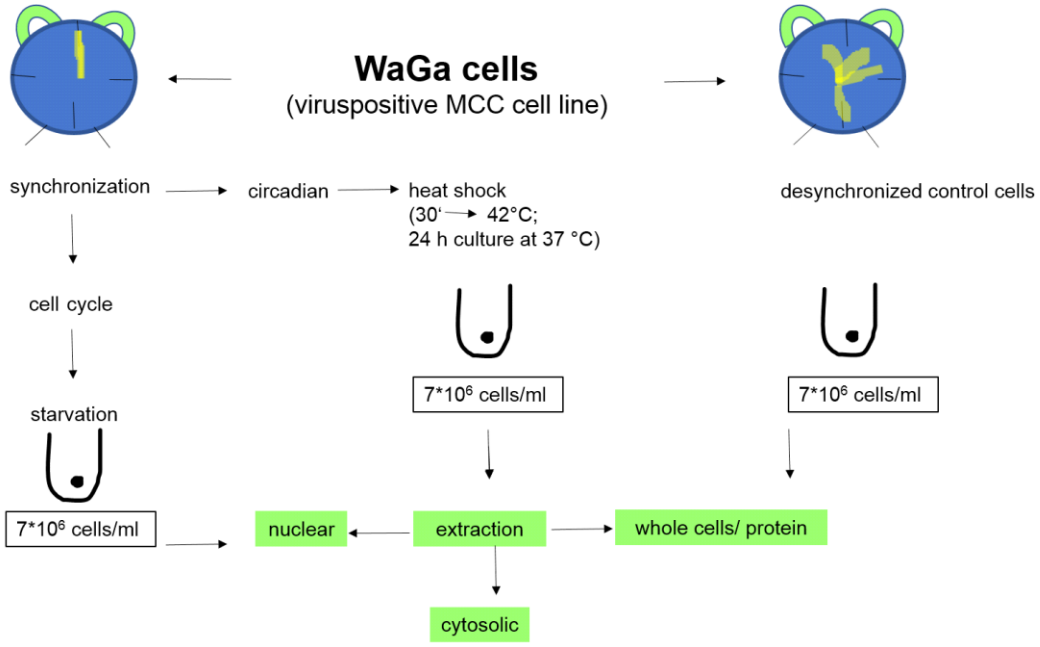

Fig. 8: An illustration of the overall experimental design concerning nuclear and cytosolic extraction of MCPyV-positive WaGa cells as well as whole cell lysates destined for either cell cycle or circadian synchronization.

5.2 Considerations regarding the Experimental Outcome

Cell culture and determination of protein concentration. Unfortunately, in case of two cell lines, namely MCC 13 and MKL2, the growth performance was not meeting the expectations and demand. Therefore, a low output in sample fractions was achieved. As indicated by the labeling of Fig. 4, where the results of the western blot regarding the expression pattern of anti-PTEN including thirteen MCC cell lines is presented, the amount of sample loaded was 25 µg per sample/well. This is also valid for the amount loaded of the Western blot represented in Fig. 5, where only twelve MCC cell lines were investigated since the MCC cell line MKL 2 was not available for short-term experimental processing. Additionally, to exploit the available wells for possible loading, another 25-µg sample had been loaded, precisely heat-shocked whole cell lysate of WaGa cells. The relative protein expressions were determined by using densitometry and the program ImageLab.

Loading control. In both experimental strategies, anti-β-Tubulin antibody was employed. Obviously concerning the anti-PTEN expression Western blot series, there is a reduced intensity of sample MCC 13 represented in figure 5, probably due to a spill

out or misloading or loss of protein, even a miscalculation of protein concentration must be noted as a possible but unlikely reason. All the other samples seem to be quite evenly in intensity as expected. This counts as well for the second experimental set-up nuclear and cytoplasmic fractionation. Here, anti-β-Tubulin is used as a cytosolic loading control. Therefore, expression of bands in quite similar intensity are only appearing in the whole cell lysate samples as well as in the cytoplasmic samples as shown in Fig. 7. Additionally, also anti-β-actin antibody was successfully used as a cytosolic loading control as shown in Fig. 6. As a nuclear control anti-Lamin B1 antibody had been chosen. Despite the predicted and observed band sizes of 66 kDa and 68 kDa, obtained from the product datasheet of abcam, double bands were observed for the whole cell lysate as well as nuclear extract samples at around 65 kDa and 70 kDa as shown in Fig. 7. One might consider degradation processes, which seems not likely. As furthermore stated in the data sheet provided by abcam it is mentioned in the section general notes that Lamin B1 is cleaved in apoptotic cells by caspases.[88,91] Another aspect for discussion might be the possibility of isoforms. In case of Lamin B1 there are two transcript variants reported. Thus, one of the resulting proteins is shorter compared to the other one.[92] Also notable is the fact that there is a difference in expression intensity between the whole cell lysate samples and the nuclear extraction samples indicating a sufficient but not strong efficiency in extracting the nuclear fractions. Although, apart from the cytoplasmic extraction sample treated by heat-shock, no band showed up regarding the cytoplasmic WaGa samples of the Western blot of Fig. 7 (Lamin B1; upper gel) and the non-heat-shock cytoplasmic sample of the Western blot represented in Fig. 7 (Lamin B1; lower panel). This aforementioned single band of the upper gel at around 65 kDa of the cytoplasmic extraction sample could be a spill over in the process of actual loading or other experimental errors.

Control samples. Although the actual experimental performance was not involving time -dependent analyses as required in the experimental strategy with the aim to investigate circadian oscillation aspects of key regulatory proteins with the ability to shuttle between different cellular compartments. Nevertheless, the fundamental basis for further experiments was established. Moreover, in congruence to meet the requirements of equal treatment, all three experimental conditions of the experimental set-up nuclear and cytoplasmic extraction, namely whole PE, NE and CE, were

differentiated into two distinct samples each, either heat-shock treated or synchronized and untreated or desynchronized. In this particular series of single time point experiments, no significant difference between heat-shocked and untreated samples can be seen. This has to be addressed in future experiments.

5.3 Optimization suggestions concerning experimental procedure

Regarding the Western blot result where AKT was probed as shown in Fig. 4, it can be noted that the bands including WaGa, MKL 1, MKL 2, PeTa, AsTi and WoWe 2 samples are slightly less intense compared to the remaining samples loaded into wells on the far right and left side of the gel. The sealing process and the subsequent incubation of the nitrocellulose membrane with the antibody of interest might explain this. If against every good intention and careful handling, any air bubble, even a tiny one, remains in the sealed plastic foil package including the nitrocellulose membrane incubated with the antibody, such a typical expression intensity pattern might be possible. During the incubation on a rotating platform, the liquid collects on the bottom due to gravitation but the edges of the foil might coil up slightly, due to the capillary effect; enough that any remaining air bubbles will be located in the middle and top side of the foil package. Ideally, to avoid any bubbles, the membrane should be incubated in the smallest possible tray saturated and covered completely by the antibody solution. Due to the intention to waste as little antibody material as possible, the sealed plastic foil solution was strongly recommended. Additionally, according to this concern, each membrane had been cut as small as possible after the Ponceau S Red staining.

Moreover, the experimental set-up could be adapted or optimized as for example by including sonication as a procedure to a more successful cell lysis, thus disruption of cell membranes. Importantly, if applied, it should be taken care of excessive heat development by keeping the samples constantly on ice water.

5.4 Is MCPyV-positivity making the difference?

The work of Hafner *et al*. might be giving hope for the accuracy of the initial hypothesis that an inactivation, may it be an inactivation of the tumor suppressor PTEN, is involved in the pathogenesis of MCC. [23] Another important aspect is the question whether viral

antigens are actively involved in the activation of the PI3K/AKT pathway. This hypothesis is based on the fact that the polyomavirus Simian Virus (SV) 40's encoded LTAg induces the PI3K/AKT pathway via it's interaction with the insulin receptor substrate 1. In case of the sTAg, this is accomplished via inhibition of protein phosphatase 2A. In brief, Hafner *et al*. probed amongst other antibodies anti-pAKT^{S473} and pAKT^{T308} in a Western blot analysis including total cell lysates of seven MCPyV-positive as well as three MCPyV-negative MCC cell lines. These authors have clearly demonstrated that silencing (by shRNAs) of the TA was without effects on activating AKT phosphorylation indicating that AKT activation is independent of MCPyV T antigens in MCC cells. Moreover, immunohistochemical staining of tissue microarrays containing 41 MCC samples revealed in 88% a strong or very strong staining for pAKT^{T308}. [23] These data are in line with results from my own study that are shown in Figs. 4 and 5.

Moreover, in a SNaPshot-based tumor genotyping study of 60 primary MCC samples 13 cancer gene mutations were analyzed by Nardi *et al*..[22] These authors performed also immunoblotting experiments where two out of three MCPyV-positive MCC cell lines (including MKL1 and MKL2) used in their study, showed no PI3K/AKT pathway activation. This coincides with the results of this thesis as indicated by Fig. 4, where MKL 2 is showing no immunoreactive band, and MKL 1 is revealing a weak signal expressed by a faint band. Despite, all their three MCPyV-negative cell lines appeared to have a strong activation regarding pAKT^{S473} and pAKT^{T308}. Amongst the MCPyV-negative cell lines employed in this study only MCC 26 was revealing a strong activation. Furthermore, the authors suggested that the absence of MCPyV in phosphatidylinositol-4,5-bisphosphate 3-kinase catalytic subunit α (PIK3CA)-mutant MCCs indicates alternative oncogenic mechanisms for tumorigenesis, which in turn would explain the overall better outcome of MCPyV-positive cases.[22] As already described above, no pronounced differences in PTEN expression were observed between MCPyV-positive and MCPyV-negative MCC samples.

5.5 PTEN, in constant suspicion of loss of function, truly counts for all cancers

Although, a plethora of mutational analyses regarding MCC were performed and reported, the pathogenesis of MCC is still not thoroughly understood. It is, however, suspected and partly demonstrated that in MCPyV-negative MCC cells somatic genetic mutations play a greater role in pathogenesis than in those MCC cells, which harbor viral DNA.

The literature describes unique differences in chromosomal abnormalities, genetic mutations, expression profiles and epigenetic control of individual tumors thus several molecular abnormalities appear to be associated with MCC.[93]

Among the most common are tumor suppressor anomalies such as tumor protein TP53, Rb1 and suppressor of fused homolog SUFU. Next-generation sequencing analysis of 17 MCC patient samples published by Cohen *et al*. revealed that the TP53 locus harbors the most common genetic anomaly.[94] Hafner *et al*. pointed out that mutations in tumor suppressor genes such as TP53, TP73 and CDKN2A occur only in a limited number of MCCs.[23] On the other hand, overexpression of Hedgehog (Hh) signal pathway proteins, telomerase activation (telomerase reverse transcriptase TERT) and tyrosine kinase signaling activation (AKT, Kit, platelet-derived growth factor receptor α (PDGFR α), phosphatidylinositol-4,5-bisphosphate 3-kinase catalytic subunit α (PIK3CA) and also PTEN) are reported.[93,94]

PTEN mutations/alterations are frequently observed in a variety of human tumors.[32,33,34,35,36,37,38,39] Despite a high frequency of LOH at 10q23, only one tumor out of 26 tumor samples obtained from 23 MCC patients tested via mutation and homozygous deletion screening by Van Gele *et al*., showed a nonsense mutation and another one a homozygous deletion of exon 9 in the PTEN gene.[78] PTEN-positive cells were only recognized in a low percentage of cells by immunohistochemical studies presented by Ferdinandez *et al*. but in one case of MCC, 'strong and diffuse' PTEN expression was observed. Furthermore, they stated that in their MCC cohort downregulation of PTEN might contribute to an overexpression of survivin, which is overexpressed in various cancers and thus was highly expressed in the nucleus of MCC cells. Moreover, they conclude that survivin seems to be less involved in metastasis than in the MCC development.[11] As also mentioned by Hafner *et al*., despite

the low incidence of PTEN mutations in MCC, a lack of PTEN protein expression is frequently observed.[23]

My own Western blot data obtained from MCPyV-positive and MCPyV-negative cell lines revealed strong and intense PTEN signals (Fig. 4 and 5). Following separation and isolation of nuclei revealed that at least in WaGa cells PTEN appears to be exclusively located in the nuclear compartment (Fig. 7). This is of importance for a potential effect on circadian rhythm since also CLOCK was exclusively detected in the nucleus (Fig. 7) which is in line with available literature evidence.

6. Conclusion and Perspective

In summary, I could show that all cell lines tested during the present thesis express PTEN and display at least some extent of AKT activation. In WaGa cells, (no other MCC cells were tested) PTEN and CLOCK were detected exclusively in the nucleus. As reported in literature, inactivating mutations of PTEN are a rare event in MCC although; a deficiency in PTEN protein expression was reported.[11] These findings are not in agreement with the results of immunoblot analyses performed here where all cell lines studied express detectable levels of PTEN. Hafner *et al.* reported that amongst loss of PTEN, the PI3K/AKT pathway could be activated by alternative pathway including oncogenic mutations.[23] Furthermore, as discussed by Van Gele *et al*., other tumor suppressor genes at chromosome 10 could be involved in MCC tumorigenesis. Moreover, an inactivation of the PTEN gene might not be associated with MCC development.[78] If alternative mechanisms are actively implicated in MCC pathogenesis, remains to be seen.

Although I could demonstrate that both, PTEN and CLOCK are detectable solely in nuclear extracts (Fig. 6 and 7) the question of an altered molecular circadian mechanism in MCC cells remains fully open. Of particular interest are potential differences between viral-associated MCC cells and MCPyV-negative MCC cells. There is still a wide field for discoveries in MCC chronotherapeutic aspects to be made until an effective therapy is ready to offer promising benefits such as a specifically targeted high-dose therapy at distinct time points with fewer side effects amongst efficacy.

7 Bibliography

1. Toker C. (1972). „Trabecular Carcinoma of the Skin *Arch Dermatol.* **105**(1): pp. 107- 110; doi:10.1001/archderm.1972.01620040075020.

2. Bolognia, Jean L., Jorizzo Joseph L. & Schaffer Julie V.(2009). '*Dermatology'*; Volume **2**, 3rd edition; Elsevier Health Sciences, London; pages 1954-1955.

3. Becker, J.C. (2010). „Merkel cell carcinoma. "*Annals of Oncology*, Volume **21**, Issue suppl_7: pages vii81–vii85.

4. Tang C.K. & Toker C. (1978). „Trabecular carcinoma of the skin: an ultrastructural study." *Cancer*;**42**(5); pp. 2311-21.

5. Nghiem Paul, Kaufman Howard L., Bharmal Murtuza, Mahnke Lisa, Phatak Hemant & Becker Jürgen C. (2017). „Systematic literature review of efficacy, safety and tolerability outcomes of chemotherapy regimens in patients with metastatic Merkel cell carcinoma." *Future Oncol.*, **14**; pp. 1263-1279. doi:10.2217/fon-2017-0072.

6. Moll I., Roessler M., Brandner J. M., Eispert A. C., Houdek P., & Moll R. (2005). „Human Merkel cells- aspects of cell biology, distribution and functions." *European journal of cell biology*; **84**(2-3); pp. 259-71.

7. Houben R., Schrama D. & Becker J. C. (2009). „Molecular pathogenesis of Merkel cell carcinoma." *Experimental Dermatology*; **18**: 193–198. doi:10.1111/j.1600-0625.2009.00853.x.

8. Youlden D.R., Soyer H.P., Youl P.H., Fritschi L. & Baade P.D. (2014). „Incidence and Survival for Merkel Cell Carcinoma in Queensland, Australia, 1993-2010." *JAMA Dermatol.*;**150**(8):864–872. doi:10.1001/jamadermatol.2014.124

9. Sauer C, M, Haugg A, M, Chteinberg E, Rennspiess D, Winnepenninckx V, Speel E, J, Becker J, C, Kurz A, K, & Zur Hausen A. (2017). „Reviewing the current evidence supporting early B-cells as the cellular origin of Merkel cell carcinoma." *Crit. Rev. Oncol. Hematol.*, Vol. **116**, pp. 99-105.

10. Zur Hausen, A., Rennspiess, D., Winnepenninckx, V., Speel, E.J., & Kurz, A.K. (2013). „Early B-cell differentiation in Merkel cell carcinomas: clues to cellular ancestry.", *Cancer Res.*, **73**, pp. 4982–4987.

11. Fernández-Figueras Maria-Teresa, Puig Lluis, Musulén Eva, Gilaberte Montserrat, Lerma Enrique, Serrano Sergio, Ferrándiz Carlos & Ariza Aurelio. (2007). „Expression profiles associated with aggressive behavior in Merkel cell carcinoma." *Modern Pathology;* **20** (1): pp. 90-101.

12. Guy Jr. G., Thomas C., Thompson T., Watson M., Massetti G., & Richardson L. (2015). „Vital signs: melanoma incidence and mortality trends and projections - United States, 1982-2030.“ *MMWR: Morbidity & Mortality Weekly Report*, Vol. **64**, No. 21, pp. 591-596.

13. Costa A., Mackelfresh J., Gilbert L, Bonner M., Y., & Arbiser J., L. (2017). „Activation of Protein Kinase C ε in Merkel Cell Polyomavirus–Induced Merkel Cell Carcinoma.“ *JAMA Dermatol.*; **153**(9): pp. 931–932. doi:10.1001/jamadermatol.2017.1296

14. Hodgson Nicole C. (2005). „Merkel Cell Carcinoma: Changing Incidence Trends.“ *Journal of Surgical Oncology*; **89**: pages 1–4.

15. Ullrich S, E., & Byrne S, N. (2012). „The Immunologic Revolution: Photoimmunology.“ *The Journal of Investigative Dermatology*, **132**(3 0 2), pp. 896–905. http://doi.org/10.1038/jid.2011.405

16. Read Scott A., and Douglas Mark W. (2014). „Virus induced inflammation and cancer development.“ *Cancer Letters*; **345**; pp. 174-181.

17. Houben Roland, Shuda Masahiro, Weinkam Rita, Schrama David, Feng Huichen, Chang Yuan, Moore Patrick S., & Jürgen C. Becker Jürgen C. (2010). „Merkel Cell Polyomavirus-Infected Merkel Cell Carcinoma Cells Require Expression of Viral T Antigens.“ *JOURNAL OF VIROLOGY*. Vol. **84**, No. **14**; p. 7064–7072.

18. Feng Huichen, Shuda Masahiro, Chang Yuan & Moore Patrick S. (2008). „Clonal Integration of a Polyomavirus in Human Merkel Cell Carcinoma.“ *SCIENCE*; Vol. **319**.(5866); pp. 1096-1100.

19. Schrama D., Hesbacher S., Angermeyer S., Schlosser A., Haferkamp S., Aue A., Adam C., Weber A., Schmidt M. & Houben R. (2016). „Serine 220 phosphorylation of the Merkel cell polyomavirus large T antigen crucially supports growth of Merkel cell carcinoma cells.“ *International Journal of Cancer*; **138** (5); pp. 1153-1162.

20. Shuda, M., Feng, H., Kwun, H. J., Rosen, S. T., Gjoerup, O., Moore, P. S., & Chang, Y. (2008). „T antigen mutations are a human tumor-specific signature for Merkel cell polyomavirus.“ *Proceedings of the National Academy of Sciences of the United States of America*, **105**(42), pp. 16272–16277. http://doi.org/10.1073/pnas.0806526105

21. Verhaegen M. E., Mangelberger D., Weick J. W., Vozheiko T. D., Harms P. W., Nash K. T., Quintana E., Baciu P., Johnson T., M., Bichakjian C., K., & Dlugosz A. A. (2014). „Merkel Cell Carcinoma Dependence on Bcl-2 Family Members for Survival.“ *The Journal of Investigative Dermatology*, **134**(8), pp. 2241–2250. http://doi.org/10.1038/jid.2014.138

[22] Nardi Valentina, Song Youngchul, Santamaria-Barria Juan A., Cosper Arjola K., Lam Quynh, Faber Anthony C., Boland Genevieve M., Yeap Beow Y., Bergethon Kristin, Scialabba Vanessa L., Tsao Hensin, Settleman Jeffrey, Ryan David P., Borger Darrell R., Bhan Atul K., Hoang Mai P., Iafrate Anthony J., Cusack James C., Engelman Jeffrey A., & Dias-Santagata Dora. (2012). „Activation of PI3K Signaling in Merkel Cell Carcinoma." *Clin Cancer Res*.; **18**(5); pp. 1227–1236.

[23] Hafner C., Houben R., Baeurle A., Ritter C., Schrama D. and Landthaler M. (2012) „Activation of the PI3K/AKT Pathway in Merkel Cell Carcinoma." *PLoS ONE;* **7**(2): e31255. https://doi.org/10.1371/journal.pone.0031255.

[24] Kwun H., J., Chang Y., & Moore P., S. (2017). „Protein-mediated viral latency is a novel mechanism for Merkel cell polyomavirus persistence." Proc Natl Acad Sci U S A.; 114(20): E4040-E4047. doi: 10.1073/pnas.1703879114.

[25] Hanahan Douglas and Weinberg Robert A.. (2000). „The Hallmarks of Cancer." *Cell*; **100** (1); pp. 57-70.

[26] Berger Alice H., Knudson Alfred G., & Pandolfi Pier Paolo. (2011). "A Continuum Model for Tumour Suppression." *Nature* **476**; 7359: pp.163–169.

[27] Teng David H.F., Hu Rong, Lin Huai, Davis Thaylon, Iliev Diana, Frye Cheryl, Swedlund Brad, Hansen Kipp L., Vinson Vickie L., Gumpper Kathryn L., Ellis Lee, El-Naggar Adel, Frazier Marsha, Jasser Samar, Langford Lauren A., Lee Jeff, Mills Gordon B., Pershouse Mark A., Pollack Raphael E., Tornos Carmen, Troncoso Patricia, Yung Alfred W.K., Fujii Gregory, Berson Amy, Bookstein Robert, Bolen Joseph B., Tavtigian Sean V., & Steck Peter A. (1997). „*MMAC1/PTEN* Mutations in Primary Tumor Specimens and Tumor Cell Lines." *Cancer Res*; **57**; (23); pp. 5221-5225.

[28] Lodish H, Berk A, Zipursky S, L, et al. (2013). Molecular Cell Biology, 7th edition; chapter 24.2 Genetic Basis of Cancer, New York: Freeman W., H.; pp. 1128-1129.

[29] Huse J.T., Brennan C., Hambardzumyan D., Wee B., Pena J., Rouhanifard S. H., Sohn-Lee C., Agami R., Tuschl T., & Holland E.C. (2009). „The PTEN-regulating microRNA miR-26a is amplified in high-grade glioma and facilitates gliomagenesis in vivo." Genes Dev.; 23 (11); pages 1327-37. doi: 10.1101/gad.1777409.

[30] Alberts Bruce, Johnson Alexander, Lewis Julian, Raff Martin, Roberts Keith & Walter Peter. (2002). *Molecular Biology of The Cell*, **4**th edition; Garland Science; pages 1337 and 1339.

[31] Carracedo A., Alimonti A., & Pandolfi P. P. (2011). 'PTEN level in tumor suppression: How much is too little?', *Cancer Research*, **71**(3), pp. 629–633. http://doi.org/10.1158/0008-5472.CAN-10-2488

[32] Herbst R.A., Weiss J., Ehnis A., Cavenee W.K., & Arden K.C. (1994). „Loss of heterozygosity for 10q22-qter in malignant melanoma progression." *Cancer Res*. **54**; pp. 3111-3114.

[33] Rempel S.A., Schwechheimer K., Davis R.L., Cavenee W.K., & Rosenblum M.L. (1993). „Loss of heterozigosity for loci on chromosome 10 is associated with morphologically malignant meningioma progression." *Cancer Res*. **53**, 2386-2392.

[34] Morita R. et al. (1991). „Common regions of deletion on chromosomes 5q, 6q, and 10q in renal cell carcinoma." *Cancer Res*. **51**; pp. 5817-5820.

[35] Eagle L.R. et al. (1995). „Mutation of the MXI1 gene in prostate cancer." *Nature Genet*. **9**; pp. 249-255.

[36] Peterson I. et al. (1997). „Small-cell lung cancer is characterized by a high incidence of deletions on chromosomes 3p, 4q, 5q, 10q, 13q, and 17p." *Brit. J. Cancer* **75**; pp. 79-86.

[37] Peiffer S.L. et al. (1995). „Allelic loss of sequences from the long arm of chromosome 10 and replication errors in endometrial cancers." *Cancer Res*. **55**; pp.1922-1926.

[38] Gray I.C. et al. (1995). „Loss of chromosomal region 10q23-25 in prostate cancer." *Cancer Res*. **55**; pp. 4800-4803.

[39] Trybus T.M., Burgress A.C., Wojno K.J., Giover T.W., & Macoska J.A. (1996). „Distinct areas of allelic loss on chromosomal regions 10p and 10q in human prostate cancer." *Cancer Res*. **56**; pp. 2263-2257.

[40] https://www-1ncbi-1nlm-1nih-1gov-1pubmed.han.medunigraz.at/pubmed/?term=PTEN+and+mutation (12.10.2017)

[41] https://www-1ncbi-1nlm-1nih-1gov-1pubmed.han.medunigraz.at/pubmed/?term=PTEN+and+loss (12.10.2017)

[42] Shi Y, Paluch B, E, Wang X., & Jiang, X. (2012). „PTEN at a glance." *Journal of Cell Science*, **125**(20), pp. 4687–4692. http://doi.org/10.1242/jcs.093765

[43] https://www-1ncbi-1nlm-1nih-1gov-1pubmed.han.medunigraz.at/pubmed/?term=PTEN+and+Merkel+cell+carcinoma (12.10.2017)

44. http://www.genenames.org/cgi-bin/gene_symbol_report?hgnc_id=HGNC:9588 (12.09.2017)

45. Li J., Yen C., Liaw D., Podsypanina K., Bose S., Wang S.I., Puc J., Miliaresis C., Rodgers L., McCombie R., Bigner S.H., Giovanella B.C., Ittmann M., Tycko B., Hibshoosh H., Wigler M.H., & Parsons R. (1997). „PTEN, a putative protein tyrosine phosphatase gene mutated in human brain, breast, and prostate cancer." *Science*; **275** (5308); pp.1943-1947.

46. Hollander M.C., Blumenthal G.M., & Dennis P., A. (2011). „PTEN loss in the continuum of common cancers, rare syndromes and mouse models." *Nat Rev Cancer*. Apr;**11** (4); pp. 289-301. doi: 10.1038/nrc3037.

47. Collaud S., Tischler V., Atanassoff A., Wiedl T., Komminoth P., Oehlschlegel C., Weder W., & Soltermann A. (2015). „Lung neuroendocrine tumors: correlation of ubiquitinylation and sumoylation with nucleo-cytosolic partitioning of PTEN." *BMC Cancer*, **15**; p. 74. http://doi.org/10.1186/s12885-015-1084-5.

48. Zhang j., Grindley J., C., Yin T., Jayasinghe S., He X., C., Ross J., T., Haug J., S., Rupp D., Porter-Westpfahl K., S., Wiedemann L., M., Wu H., & Li L. (2006), „PTEN maintains haematopoietic stem cells and acts in lineage choice and leukaemia prevention." *Nature*, **441**(7092): pp. 518-22.

49. Lodish H, Berk A, Zipursky S, L, *et al*. (2013). '*Molecular Cell Biology',* **7**th edition; chapter **24.4** Cancer and Mutation of Cell Division and Checkpoint Regulators, New York: Freeman W, H, p. 1143.

50. Steck P. A., Pershouse M. A., Jasser S. A., Yung W. K. A., Lin H., Ligon A. H., Langford L. A., Baumgard M. L., Hattier T., Davis T., Frye C., Hu R., Swedlund B., Teng D. H. F., & Tavtigian S. V. (1997) „Identification of a candidate tumor suppressor gene, MMACl, at chromosome l0q23.3 that is mutated in multiple advanced cancers." *Nat. Genet*.; **15**; pp. 356-362.

51. Van Gele M., Speleman F., Vandesompele J., Van Roy N., & Leonard J. H. (1998). Characteristic pattern of chromosomal gains and losses in Merkel cell carcinoma detected by comparative genomic hybridization." *Cancer Res*.; **58**: pp. 1503–1508.

52. Husse, J, Eichele, G, & Oster, H. (2015). „Synchronization of the mammalian circadian timing system: Light can control peripheral clocks independently of the SCN clock: Alternate routes of entrainment optimize the alignment of the body's circadian clock network with external time." *Bioessays*, **37**(10), pp. 1119–1128.

[53.] Kettner N. M., Katchy C.A., & Fu L. (2014). „Circadian gene variants in cancer.“ *Annals of medicine*; **46**(4); pp. 208-220. doi:10.3109/07853890.2014.914808.

[54.] Fu Loning & Lee Cheng Chi. (2003). „The circadian clock: pacemaker and tumour suppressor.“ *Nature Revies Cancer* **3**, pages 350-361; doi:10.1038/nrc1072.

[55.] Sancar A, Lindsey-Boltz L, A, Gaddameedhi S, Selby C, P, Ye R, Chiou Y, Y, Kemp M, G, Hu J, Lee J, & Ozturk N. (2014). „Circadian Clock, Cancer, and Chemotherapy“, *Biochemistry*, **54**(2); pp.110-123.

[56.] Plikus M. V., Van Spyk E. N., Pham K., Geyfman M., Kumar V., Takahashi J. S., & Andersen B. (2015). „The circadian clock in skin: implications for adult stem cells, tissue regeneration, cancer, aging, and immunity.“ *Journal of Biological Rhythms*, **30**(3); pp. 163–182. http://doi.org/10.1177/0748730414563537 (2015).

[57.] Aguilar-Arnal Lorena & Paolo Sassone-Corsi. (2015). “Chromatin Landscape and Circadian Dynamics: Spatial and Temporal Organization of Clock Transcription.” *Proceedings of the National Academy of Sciences of the United States of America* **112**; 22; pp. 6863–6870.

[58.] Koike N., Yoo S.-H., Huang H.-C., Kumar V., Lee C., Kim T.-K., & Takahashi J. S. (2012). „Transcriptional Architecture and Chromatin Landscape of the Core Circadian Clock in Mammals.“ *Science (New York, N.Y.)*, **338** (6105); pp. 349–354. http://doi.org/10.1126/science.1226339

[59.] Smarr B. L., Jennings K. J., Driscoll J. R., & Kriegsfeld L. J. A. (2014). „Time to Remember: The Role of Circadian Clocks in Learning and Memory.“ *Behavioral Neuroscience*, **128**(3), 283–303. http://doi.org/10.1037/a0035963

[60.] Altman B.J. (2016). „Cancer Clocks Out for Lunch: Disruption of Circadian Rhythm and Metabolic Oscillation in Cancer.“ *Frontiers in Cell and Developmental Biology*; **4**; p. 62. doi:10.3389/fcell.2016.00062.

[61.] Iwamoto A, Kawai M, Furuse M, & Yasuo S. (2014). „Effects of chronic jet lag on the central and peripheral circadian clocks in CBA/N mice.“ *Chronobiology international*; **31**(2); pp. 189-98.

[62.] Wong P. M., Hasler B. P., Kamarck T. W., Muldoon M. F., & Manuck S. B. (2015). „Social Jetlag, Chronotype, and Cardiometabolic Risk.“ *The Journal of Clinical Endocrinology and Metabolism*, **100**(12); pp. 4612–4620. http://doi.org/10.1210/jc.2015-2923

[63.] Fu L., & Kettner N. M. (2013). „The Circadian Clock in Cancer Development and Therapy.“ *Progress in Molecular Biology and Translational Science*, **119**; pp. 221–282. http://doi.org/10.1016/B978-0-12-396971-2.00009-9

64. Gérard C., & Goldbeter, A. (2012). „Entrainment of the Mammalian Cell Cycle by the Circadian Clock: Modeling Two Coupled Cellular Rhythms.“ *PLoS Computational Biology*, **8**(5), e1002516. http://doi.org/10.1371/journal.pcbi.1002516

65. Bieler J., Cannavo R., Gustafson K., Gobet C., Gatfield D., & Naef F. (2014). „Robust synchronization of coupled circadian and cell cycle oscillators in single mammalian cells.“ *Molecular Systems Biology*, **10**(7), p. 739. http://doi.org/10.15252/msb.20145218

66. Chaix A., Zarrinpar A., & Panda S. (2016). „The circadian coordination of cell biology.“ *The Journal of Cell Biology*, **215**(1), pp. 15–25. http://doi.org/10.1083/jcb.201603076

67. Lodish Harvey, Kaiser Chris A., Bretscher Anthony, Amon Angelika, Berk Arnold, Krieger Monty, Ploegh Hidde and Scott Matthew P.. (2013) „*Molecular Cell Biology*.“ **7**th edition; chapter **19** The Eukaryotic Cell Cycle, New York: Freeman W, H, pp. 873-876 and 906.

68. Matsumoto Camila S., Almeida Luciana O., Guimarães Douglas M., Martins Manoela D., Papagerakis Petros, Papagerakis Silvana, Leopoldino Andreia M., Castilho Rogerio M. & Squarize Cristiane H. (2016). „PI3K-PTEN dysregulation leads to mTOR-driven upregulation of the core clock gene BMAL1 in normal and malignant epithelial cells.“ *Oncotarget*, Vol. **7**, No. 27; pp. 42393-42407.

69. Miki Takao, Zhao Zhaoyang & Lee Cheng Chi. (2016). „Interactive Organization of the Circadian Core Regulators PER2, BMAL1, CLOCK and PML.“ *Scientific Reports*. **6**: p. 29174. doi: 10.1038/srep29174.

70. Leonard J. H., Ramsay J. R., Kearsley J. H., & Birrell G. W. (1995). „Radiation sensitivity of Merkel cell carcinoma cell lines.“ *Int. J. Rad. Oncol. Biol. Phys*., **32**: 1401-1407.

71. Van Gele M., Leonard J. H., Van Roy N., Van Limbergen H., Van Belle S., Cocquyt V., Salwen H., De Paepe A., & Speleman F. (2002). „Combined karyotyping, CGH and M-FISH analysis allows detailed characterization of unidentified chromosomal rearrangements in Merkel cell carcinoma.“ *Int. J. Cancer*; **101**; pp. 137–145. doi:10.1002/ijc.10591

72. Houben R., Dreher C., Angermeyer S., Borst A., Utikal J., Haferkamp S., Peitsch W., K., Schrama D., & Hesbacher S. (2013). „Mechanisms of p53 Restriction in Merkel Cell Carcinoma Cells Are Independent of the Merkel Cell Polyoma Virus T Antigens.“ *Journal of Investigative Dermatology*; **133** (10): pp. 2453-2460.

[73.] https://www.merkelcell.org/news-and-publications/2015/summary-of-10th-annual-mmig-meeting/ (24.09.2017).

[74.] Racki W., J., Covassin L., Brehm M., Pino S., Ignotz R., Dunn R., Laning J., Graves S., K., Rossini A., A., Shultz L., D., & Greiner, D. L. (2010). „NOD-*scid IL2rγ^{null}* (NSG) Mouse Model of Human Skin Transplantation and Allograft Rejection.“ *Transplantation*, **89**(5), pp. 527–536. http://doi.org/10.1097/TP.0b013e3181c90242

[75.] https://www.jax.org/strain/001303 (07.10.2017)

[76.] https://en.wikipedia.org/wiki/NOD_mice (07.10.2017)

[77.] Paulson Kelly G., Tegeder Andrew, Willmes Christoph, Iyer Jayasri G., Afanasiev Olga K., Schrama David, Koba Shinichi, Thibodeau Renee, Nagase Kotaro, Simonson William T., Seo Aaron, Koelle David M., Madeleine Margaret, Bhatia Shailender, Nakajima Hideki, Sano Shigetoshi, Hardwick James S., Disis Mary L., Cleary Michele A., Becker Jürgen C., & Nghiem Paul. (2014). „Downregulation of MHC-I Expression Is Prevalent but Reversible in Merkel Cell Carcinoma.“ *Cancer Immunol Res.*; **2** (11); pp. 1071–1079.

[78.] Van Gele M., Leonard J., H., Van Roy N., Cook A., L., De Paepe A., & Speleman F. (2001). „Frequent allelic loss at 10q23 but low incidence of PTEN mutations in Merkel cell carcinoma.“ *Int J Cancer*; **92**: pp. 409–413.

[79.] Claude A. (1946). „Fractionation of mammalian liver cells by differential centrifugation: I. Problems, methods, and preparation of extract.“ *J Exp Med*; **84**: pp. 51–59.

[80.] Dignam J.D., Lebovitz R.M. & Roeder R.G. (1983). „Accurate transcription initiation by RNA polymerase II in a soluble extract from isolated mammalian nuclei.“ *Nucleic Acids Research*; **11**(5):1475-1489.

[81.] Jansohn M. (2007). ‚Gentechnische Methoden.‘ **4**. Auflage; *Elsevier GmbH*; page 435.

[82.] Miskolci V., Hodgson L., Cox D., & Vancurova I. (2014). „Western Analysis of Intracellular Interleukin-8 in Human Mononuclear Leukocytes.“ *Methods in Molecular Biology (Clifton, N.J.)*, **1172**, pp. 285–293. http://doi.org/10.1007/978-1-4939-0928-5_26

[83.] Leslie N, R, Bennett D, Gray A, Pass I, Hoang-Xuan K, & Downes C, P. (2001). „Targeting mutants of PTEN reveal distinct subsets of tumour suppressor functions.“ *Biochemical Journal*, **357**(Pt 2), pp. 427–435.

[84.] Clark D, P, & Pazdernik N, J. (2013), '*Molecular Biology*', **2**nd edition, Academic Press, an imprint of Elsevier, chapter 15, Proteomics: The Global Analysis of Proteins, pp. 465-466.

85. Polyak K., & Meyerson M. (2003). ‚Gene Expression: Protein Analysis.' In: Kufe DW, Pollock RE, Weichselbaum RR, et al., editors. *Holland-Frei Cancer Medicine*. **6**th edition. Hamilton (ON): BC Decker.

86. Voet Donald & Voet Judith G. (2004). ‚Biochemistry'; 3rd edition; Wiley International Edition; page 148.

87. Delves P., J., Martin S., J., Burton D., R., & Roitt I., M. (2011). '*Roitt's Essential Immunology*', **12**th edition; Wiley-Black Well; p. 158.

88. https://www.cellsignal.com/products/primary-antibodies/lamin-b1-d4q4z-rabbit-mab/12586 (28.09.2017)

89. http://www.bio-rad.com/webroot/web/pdf/lsr/literature/Bulletin_6360.pdf (01.10.2017)

90. Sancar A., Lindsey-Boltz L., A., Gaddameedhi S., Selby C., P., Ye R., Chiou Y.-Y., Kemp M., G., Hu J., Lee J., H., & Ozturk, N. (2015). „Circadian Clock, Cancer, and Chemotherapy." *Biochemistry*, **54**(2), pp. 110–123. http://doi.org/10.1021/bi5007354

91. http://www.abcam.com/Lamin-B1-antibody-Nuclear-Envelope-Marker-ab16048.html (28.09.2017)

92. https://www.ncbi.nlm.nih.gov/gene/4001 (28.09.2017)

93. Erstad D. J., & Cusack J. C. (2014). „Mutational Analysis of Merkel Cell Carcinoma." *Cancers*, **6**(4), pp. 2116–2136. http://doi.org/10.3390/cancers6042116

94. Cohen P. R., Tomson B. N., Elkin S. K., Marchlik E., Carter J. L., & Kurzrock R. (2016). „Genomic portfolio of Merkel cell carcinoma as determined by comprehensive genomic profiling: implications for targeted therapeutics." *Oncotarget*, **7**(17), pp. 23454–23467. http://doi.org/10.18632/oncotarget.8032